BOND DISSOCIATION ENERGIES IN SOME ALKYLSILANES

A Thesis presented by,

Charles Alfred Lambert

for the degree of,

Doctor of Philosophy

in the

University of Leicester

Department of Chemistry

University of Leicester

July, 1969.

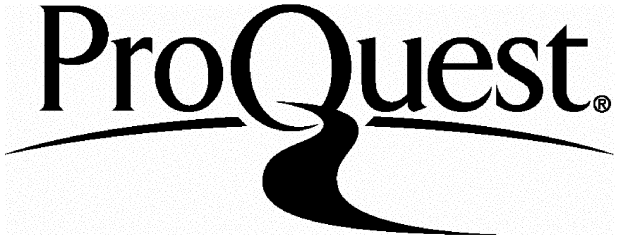

STATEMENT

The experimental work described in this thesis was carried out by the author in the Department of Chemistry of the University of Leicester, between September 1966 and July 1969.

The work has not been presented, and is not being concurrently presented for any other degree.

July, 1969.

SIGNED C A Lambert

ACKNOWLEDGEMENTS

Above all, I wish to thank my supervisor, Dr. Iain M. T. Davidson, for his unselfish help at all times, in giving me an excellent training in scientific method and problem solving.

Research is often a team effort and so I wish to thank all those who have played a part in this, and in particular, Mr. M. Jones for the many helpful discussions on mass spectrometry.

The award of a maintenance grant from S.R.C. is also gratefully acknowledged.

ABSTRACT

Appearance Potential (A.P.) measurements were carried out on the organosilanes Me_3SiX, where X = Me_3Si, Me_2SiH, Me, and H, using an automatic method with high sensitivity to concentrate on the threshold region of the ionisation efficiency curves. The method amounted to a direct extrapolation of the 'tails' of the curves, and did not involve the assumptions of the well-established methods.

The appearance potentials have been used in conjunction with kinetic and thermodynamic data to obtain values for the bond dissociation energies and heats of formation, $D(Me_3Si - X)$ and $\Delta H_f^o(Me_3SiX)_g$.

Trimethylsilane, Me_3SiH, was pyrolysed in a flow system using a quartz stirred-flow reactor situated close to the ion source of an A.E.I. MS9 mass spectrometer. The system enabled the reaction to be monitored continuously, using the high sensitivity of the MS9.

A simple chain scheme was proposed for the formation of the products, which were found to be : hydrogen, methane, disilanes, disilamethylenes, disilacyclobutanes and small amounts of dimethyl- and tetramethyl-silanes; no polymeric products were found. The hydrogen and methane were shown to be formed by the unimolecular dissociation of (Si - H) and (Si - C) bonds respectively, with negligible contribution from the chain sequence, and the activation energies were therefore identified with $D(Me_3Si - H)$ and $D(HMe_2Si - Me)$

respectively.

There was excellent agreement between the kinetic values of bond dissociation energy and those derived from the electron impact data, enabling a reliable set of quantitative data to be put forward for the A.P., $\Delta H_f^o(Me_3SiX)_g$ and $D(Me_3Si - X)$ of the organosilanes.

CONTENTS

INTRODUCTION

The bond dissociation energy, D(X - Y), is defined theoretically[1] as the change in energy, ΔE_o^o, at the absolute zero in the ideal gas state, for the reaction:

$$XY \longrightarrow X + Y$$

the products being in their ground states. In practical terms, the enthalpy change for the reaction at normal temperature, 298°K, is essentially equal to the bond dissociation energy:

$$D(X - Y) = \Delta H = \Delta H_f(X) + \Delta H_f(Y) - \Delta H_f(XY) \quad \text{...equation 1.}$$

When D(X - Y) is determined at temperatures other than 298°K, the value of the heat capacity of the reaction will be different from its value at 298°K, and so a correction should be made to account for this. In practice, since the correction is quite small, it is often omitted, ΔH then giving the upper limit of D(X - Y).

Bond dissociation energy should be distinguished from bond energy, or as it is better described, 'average bond energy', which is the quantity that summed over all the bonds of a molecule, gives the heat of formation of that molecule from its constituent atoms, e.g. in AX_n, the bond energy, E, is:

$$E(A - X) = \frac{1}{n}\left[\Delta H_f^o(A) + n\Delta H_f^o(X) - \Delta H_f^o(AX_n)\right]$$

The determination of bond dissociation energy is of fundamental importance for an understanding of the nature and reactivity of atoms and radicals, for it gives a direct measure of the strength of the

bond between them, and hence information concerning their stability, the nature of their bonding, and the mechanism by which they may react.

Very few measurements of the energies of the bonds to silicon in organosilicon compounds have been carried out and this lack of basic information has hampered the development of quantitative organosilicon chemistry. Most recent work[2,3,4,5,6] has used kinetic and electron impact techniques to study bond dissociation energies and heats of formation and has added a certain amount of data to the literature, but has at the same time complicated matters by the many anomalies. The recent work which has the most direct bearing on the work described in this thesis, is considered in the discussion section (for a review of earlier work, see reference 7).

Experiments in this thesis,[8,9,10] have been concerned with the measurement, by kinetic and electron impact methods, of the bond dissociation energies and heats of formation of the organosilicon compounds, Me_3SiX, where X = Me_3Si, Me_2SiH, Me, and H, with the purpose of acquiring a quantitative set of data to add to the literature and to explain the discrepancies, and to provide the necessary fundamental information for any future studies, (the halogen compounds Me_3SiX, X = Cl, Br, I, have also been investigated in this laboratory).

The experimental work is described in the following section, but first a review of the most important methods available for

determining bond dissociation energy is given.

The determination of bond dissociation energies and heats of formation are complementary problems, since with eqn. 1, D(X - Y) can be calculated from heats of formation, and vice versa.

This relation has proved particularly useful for calculating the heats of formation of atoms and diatomic molecules, since the bond dissociation energies may be readily measured by absorption or emission spectra. The spectroscopic method entails identifying the vibrational energy levels of the absorption or emission spectra and extrapolating them to the point at which dissociation occurs, which with the zero point energy, $\frac{1}{2}hV_o$, (V_o = vibrational frequency, h = Planck's constant) gives a very accurate measurement of D(X - Y). Polyatomic molecules, however, give spectra which are generally too complicated to be amenable to interpretation, so that most bond dissociation energies which have been reported for these molecules have been determined by kinetic or electron impact methods.

Kinetic methods

In order to obtain a value of D(X - Y) by kinetic measurements, an accurate rate constant and Arrhenius parameters must be determined, and the rate of reaction that is measured must be identifiable with the rate, and hence enthalpy change, of the unimolecular decomposition:

$$XY \underset{E_r}{\overset{E_f}{\rightleftharpoons}} X + Y$$

where E_f and E_r are the activation energies of the forward and reverse processes respectively. The enthalpy change is given by:

$$\Delta H = \Delta E + RT = (E_f - E_r) + RT$$

where the RT term allows for the change in the number of moles, and which is approximately offset by correction which should be applied to E_f to bring it to 298°K.

Thus $\Delta H = E_f - E_r$.

The activation energy, E_r, of the radical combination is assumed to be zero, so that:

$\Delta H = E_f$ i.e. the enthalpy change = the activation energy of the unimolecular decomposition.

There is considerable evidence[11,12,13] for the validity of the assumption made above, and the exact relationship of E_f and D(X - Y) is considered in detail by Szwarc[14], who concluded that there was less than 2 kcal.mole^{-1} error even up to 1000°K.

The necessity for accuracy in the measurements was also illustrated by Szwarc[14], who showed that for $\frac{1}{T_1} - \frac{1}{T_2} = 10^{-4}$, which corresponds to a temperature range of 50° if the experiments are carried out in the vicinity of 500°K, an error of 20% in the rate constants at T_1 and T_2 would produce an error of 8 kcal. in E_f.

When the products are formed by a radical non-chain reaction, (propagation reactions do not occur, see below) their rate of formation is governed by the rate of initial formation of the radicals and hence the measured activation energy is equal to that of the unimolecular decomposition. In contrast, with a chain mechanism, such as occurs in the decomposition of most simple organic compounds, it is not possible to identify the observed activation energy with

that of the unimolecular decomposition. A simple Rice-Herzfeld[86] chain mechanism is shown below:

$$M \xrightarrow{k_1} \dot{R}_1 + \dot{R}_1' \qquad \text{(INITIATION)}$$

$$\dot{R}_1 + M \xrightarrow{k_2} R_1H + \dot{R}_2$$

$$\dot{R}_2 \xrightarrow{k_3} \dot{R}_1 + M' \qquad \text{(PROPAGATION)}$$

$$\dot{R}_1 + \dot{R}_2 \xrightarrow{k_4} M'' \qquad \text{(TERMINATION)}$$

where M is an hydrocarbon and M' an unsaturated molecule.

$$-\frac{d(M)}{dt} = \left(\frac{k_1 k_2 k_3}{2k_4}\right)^{\frac{1}{2}} (M)$$

$$E = \tfrac{1}{2}(E_1 + E_2 + E_3 - E_4)$$

$$E \ll E_1$$

(E_2 and E_3 are small compared to E_1 and $E_4 = 0$, for radical combination).

The chain process therefore gives rise to a complex rate equation, the observed activation energy is a combination of the activation energies of steps with rate constants k_1, k_2, k_3 and so cannot be identified with the unimolecular decomposition.

Reaction mechanisms can often be simplified if experiments are carried out at low percentage decomposition of M. Flow systems have been used in this respect by arranging the rates of flow so that the compound spends very little time in the reactor (contact or residence time), and carrying out the experiments in the presence of an excess of a compound that will react with the radicals in such a way as to prevent the chain reaction from occurring. Toluene has been used for

this purpose in the toluene - carrier technique[15], which essentially involves passing the compound under investigation through a heated furnace in a stream of toluene, chain reactions being prevented by removal of the reactive radicals as XH. The benzyl radicals which are formed are particularly stable and do not enter into a chain reaction but simply dimerise to form dibenzyl:

$$C_6H_5CH_3 + X\cdot = C_6H_5CH_2\cdot + XH$$

$$2C_6H_5CH_2\cdot = C_6H_5CH_2CH_2C_6H_5$$

The toluene - carrier method does have the disadvantage, however, that the bond being studied must be weaker than the weakest bond in toluene, i.e. less than 85 kcal.mole^{-1}. In practice a bond strength of 70 kcal.mole^{-1} is considered the maximum that can be determined.

Aniline has also been used[87] in a similar manner:

$$PhNH_2 + X\cdot = PhNH\cdot + XH$$

the anilino radicals then dimerise,

$$2PhNH\cdot = PhNHNHPh$$

With the advances in analytical technique such as in G.l.c. and mass spectrometry, it is now possible to carry out experiments at low percentage decomposition in static systems. So far, most studies have been concerned with complex reaction mechanisms, rather than determinations of bond dissociation energy.

A full account of all the methods of determining bond dissociation energy is given in several excellent reviews[14,16,17].

Electron Impact

The first requirement for a determination of D(X - Y) by an electron impact method is an accurately measured appearance potential (A.P.), which can then be used in conjunction with other data, as will be seen, to obtain D(X - Y).

A general review of the theory is given before the bond dissociation section, followed by a survey of the methods available for the determination of appearance potentials.

Theory

An A.P. is defined as the minimum energy which a bombarding electron must possess in order to produce a particular ion from a particular molecule i.e. it is the potential at which the ion in question makes its first appearance. The simplest case is the production of the molecule ion:

$$XY + e = XY^+ + 2e \quad \text{.....1.1}$$

where the A.P. equals the I.P. (XY). When ionisation occurs with dissociation, fragment ions are produced:

$$XY + e = X^+ + Y + 2e \quad \text{.....1.2}$$

and in this case the A.P. (X^+) is a function of the bond dissociation energy, D(X - Y), the I.P.(X), and the excess energy of the fragments:

$$A.P.(X^+) = D(X - Y) + I.P.(X) + K.E. + E.E. \quad \text{.....1.3}$$

where K.E. = excess kinetic energy

E.E. = excitational energy (vibrational, rotational and electronic)

Owing to the lack of information concerning the nature of the excess

energy, it is most often assumed to be absent:

$$A.P.(X^+) = D(X - Y) + I.P.(X) \quad \ldots\ldots\ldots\ldots\ldots\ldots 1.4$$

Some indication of the accuracy of the approximation in equation 1.4 can be gained by comparing values of heats of formation, calculated from electron impact data using equation 1.4, with values determined by other methods. The result[18] indicates that excitational energy is absent in ions formed by simple ionisation, i.e. where rearrangement processes, requiring an activation energy, are absent. There are several methods[19,20] available for determining the excess kinetic energy, however they can be avoided if conditions are chosen in accordance with an empirical observation known as Stevenson's rule[21]: for the system,

$$R_1R_2 + e = R_1^+ + R_2 + 2e$$

if I.P. $(R_1) <$ I.P. (R_2), then R_1^+ and R_2 will be formed without excess kinetic energy. The rule was formulated from Stevenson's observations on a large no. of hydrocarbons, but is now applied to a whole range of compounds, there being very few exceptions.

The ionisation process may be illustrated by the Franck-Condon Principle,[22,23] which, by considering changes in vibrational characteristics, states that the nuclear coordinates do not alter during an electronic transition; thus transitions will be represented by vertical lines linking the two potential energy curves. Possible transitions are shown in diags. 1, 1.1, 1.2. Transitions take place within the area governed by the dotted lines, in accordance with

the Principle, so that in 1 the final state will lie within the region of discreet vibrational levels of XY^+. The lowest of these transitions, the 0-0, corresponds to the adiabatic or 'true' ionisation potential and is most likely to occur when the minima of the two curves lie one above the other. As the two curves are displaced from one another, the probability of the 0-0 transition decreases, but there will always be a finite probability of it occurring, necessitating great sensitivity for its detection. The limiting case here is shown in 1.1 whereby some of the transitions lead to the formation of XY^+ in vibrationally excited states and others to dissociation. After this, as in 1.2, all transitions occur with dissociation.

The probability of a transition is proportional to the square of the overlap integral:

$$P \propto \left[M^{e_1 e_2}_{v_1 v_2} \right]^2$$

where the transition is between vibrational levels v_1, v_2, and electronic states e_1, e_2; values of probability have been determined by various graphical methods such as those of Hagstrum and Tate[24].

For simple molecules, the Franck-Condon Principle is quite adequate, but for the more complex polyatomic molecules the Principle becomes too involved to be of any practical use. Hence polyatomic molecules are treated by a statistical approach according to the Quasi-equilibrium theory[25]. Essentially the theory, using a kinetic approach, tries to relate the relative abundance of ions formed in

Diags. 1,1.1, 1.2 : Franck-Condon Transitions for the diatomic molecule .XY.

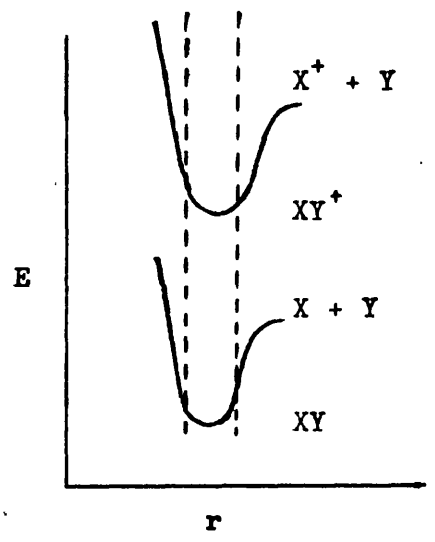

(DIAG. 1)

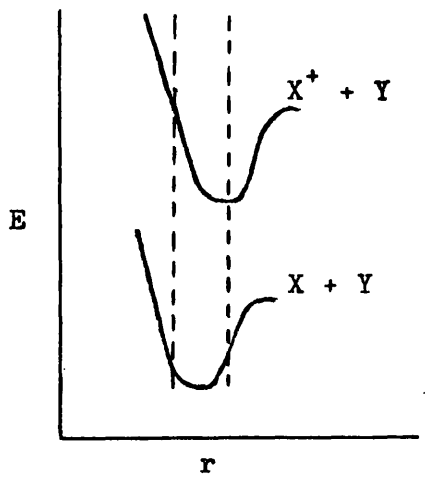

(DIAG. 1.1)

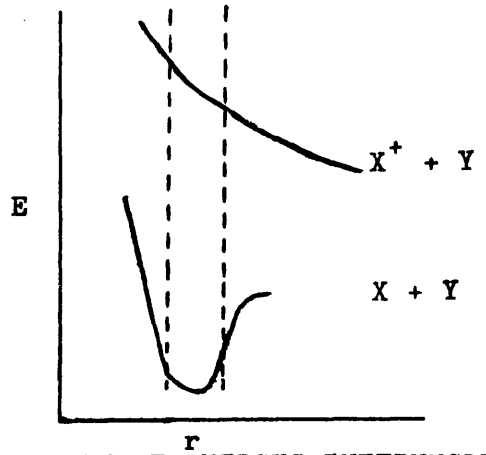

(DIAG. 1.2)

GRAPHS OF ENERGY, E, VERSUS INTERNUCLEAR DISTANCE, r.

the mass spectrometer with the strength of the bonds broken. These ions are considered to have been formed by the unimolecular decomposition of the parent ion or by some fragment. A rate scheme can therefore be set up in which, if the rate constants can be evaluated and if the competitive and parallel consecutive reactions are known, the species remaining or formed after some known time can be determined and hence the mass spectrum calculated. Although the theory is far from perfect, it does enable an insight into the formation of ions in the mass spectrometer to be achieved.

Bond Dissociation Energies

For a reliable measurement of D(X -Y) it is necessary to know:

1. The charge and excitation of the dissociation products, the quantity E.E. in eqn. 1.3 above.
2. The kinetic energies K.E. (eqn. 1.3)
3. The relevant A.P.

Then from eqns. 1.2 and 1.3, by measurement of the A.P.(X^+), taking into consideration Stevenson's rule (no excess energy), or if the excess energy is known (see the methods of Hagstrum[19] or Washburn and Berry[20]), the quantity D(X - Y) is readily obtainable as long as the I.P.(X) is known. Unfortunately, in most instances, unless X is an atom, the I.P. is not known, so that it becomes necessary to determine D(X - Y) by an indirect method. Such a method, introduced by Stevenson[21], uses thermochemical data in conjunction with the electron impact results. Thus for:

$$R_1R_2 + e = R_1^+ + \dot{R}_2 + 2e \qquad A.P.(R_1^+) = A_1$$

$$R_1H + e = R_1^+ + \dot{H} + 2e \qquad A.P.(R_1^+) = A_2$$

so that

$$R_1R_2 - R_1H = \dot{R}_2 - \dot{H} = A_1 - A_2$$

and for the hypothetical reaction,

$$R_1R_2 + 2\dot{H} = R_1H + R_2H$$

the heat of reaction ΔH_r, may be evaluated from the heats of formation of the components. Combining the equations:

$$R_2H = \dot{R}_2 + \dot{H} \quad \text{i.e.} \quad D(R_2 - H) = A_1 - A_2 - \Delta H_r$$

Alternatively, for a series of compounds PQ, PR, PS, etc., if the bond dissociation energy of one of the compounds is known, and the A.P.(P^+) is measured, then the I.P.(P) may be calculated (eqn. 1.4), and used in conjunction with the A.P.(P^+) from each of the remaining compounds to obtain their bond dissociation energies. For example, $D(Me_3Si\text{-}SiMe_3)$ determined kinetically[6], gave, in conjunction with the A.P. (Me_3Si^+) from $Me_3Si\text{-}SiMe_3$[10], a value of 7.1ev for the I.P. ($Me_3\dot{S}i$). The latter, with the A.P. (Me_3Si^+) from Me_3SiX, X = Me, H, enabled $D(Me_3Si\text{-}X)$ to be calculated for each compound[10].

The procedure outlined here is of fundamental importance in the measurement of bond dissociation energies by electron impact, because, for a series of closely related compounds, a set of self-consistent data can be obtained in which any discrepancies can be readily seen.

Equation 1.1 also links A.P. with heats of formation:

$$XY + e = X^+ + Y + 2e \qquad \text{.....1.1}$$

$$A.P.(X^+) = \Delta H_r = \Delta H^\circ_f(X^+) + \Delta H^\circ_f(Y) - \Delta H^\circ_f(XY)$$

where $\Delta H^\circ_f(X^+)$ is the standard heat of formation of the ion X^+, $\Delta H^\circ_f(Y)$ is the standard heat of formation of the radical Y, and $\Delta H^\circ_f(XY)$ is the standard heat of formation of the compound XY. The heat of formation of Y can be calculated from:

$D(X - Y) = \Delta H^\circ_f(X) + \Delta H^\circ_f(Y) - \Delta H^\circ_f(XY)$ and $\Delta H^\circ_f(X^+)$ may be obtained from

$$\Delta H^\circ_f(X^+) = I.P.(X) + \Delta H^\circ_f(X)$$

Some theoretical calculations that can be made to determine I.P. are the Equivalent Orbital method[26,27,28] and the Group orbital method[29]. The equivalent orbital approach considers that the removal of an electron from a molecular orbital distributed over the entire molecule, without disturbing the symmetry, results in ionisation. Thus there are I.P.s corresponding to each of the molecular orbitals, the I.P. being equal to the negative of the energy of the orbital. The treatment involves expressing each molecular orbital as an equivalent orbital and using a set of self-consistent I.P.s to determine, via a large determinental equation, the parameters for a particular series of compounds. The group orbital method is a modification of this for application to branched-chained hydrocarbons[26-29].

Methods of Determining Appearance Potential

The various methods available for the determination of A.P. depend upon an accurately measured ionisation efficiency curve, i.e. a plot of the ion current reaching the collector of the mass spectrometer against the energy of the ionising electrons (diag. 1.3). To achieve this the electron energy scale has to be properly calibrated, since the true electron energy can differ quite appreciably from the meter reading of the mass spectrometer, because of the presence of contact potentials in the ion source. The usual procedure is to use a standard of known I.P., quite often a noble gas atom whose I.P. has been accurately determined by other methods, such as by fitting a Rydberg series to its spectrum in the far-ultraviolet, and to measure the ionisation efficiency curves simultaneously. In this way each ion experiences similar conditions so that the problem of trying to evaluate the unknown nature of the contact potentials does not arise.

The problem of measuring the difference between the I.P. of the calibrant and the point of appearance of the ion under investigation, (and hence obtaining the A.P. of the unknown), is then just a matter of interpretation of the ionisation efficiency curves. The methods available for this are purely empirical, and even the better ones have their short-comings.

The curves have been analysed in two principal ways: the Vanishing Current[30] (or 'initial upward break') method and the

Diags. 1.3, 1.4: Ionisation Efficiency Curves

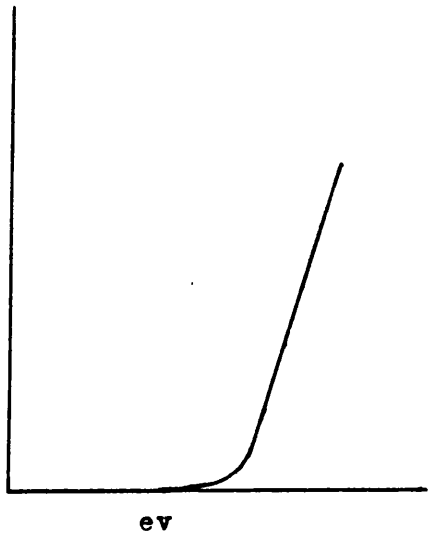

(DIAG. 1.3)

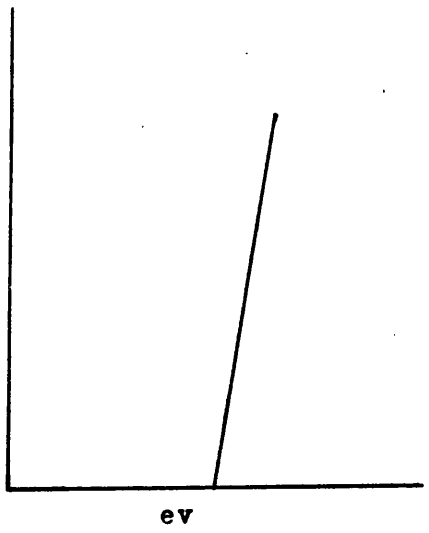

(DIAG. 1.4)

Linear Extrapolation method[31]. The other procedures, which are essentially based on these, are: the Extrapolated Voltage Difference method[32], (a modification of the vanishing current method) and logarithmic methods stemming from that of Honig's[33], and based on the linear extrapolation procedure. Another method, which attempts to reduce the energy spread of the ionising electrons, about which more will be said later, is that of Fox et al[34].

In the vanishing current method the A.P. is identified with the potential at which the ion current is first detectable, whilst in the linear extrapolation method the A.P. is taken as the point at which the extrapolated linear portion of the ionisation efficiency curve cuts the electron energy axis. Obviously the latter assumes that the process which occurs at the threshold also occurs in the region covered by the linear part of the curve, and requires that the two curves be very similar in shape. The latter requirement is quite often not found, especially when fragment ions are considered, and so this method has only very limited application (and has in fact fallen out of general use).

The vanishing current method seems more logical since it identifies the A.P. with the potential at which the ion current is first detectable, in agreement with the definition of A.P.. It is possible to derive some physical significance for the vanishing current method[35]: considering that there is a Maxwellian distribution of electron energy, the total ion current is given by,

$$I(V) = \int_{E_o}^{\infty} kn(E) \int (V + E - V_c)dE \qquad \text{where:}$$

k is a sensitivity constant, n(E)dE is the no. of electrons with thermal energy in the narrow energy range E, E + dE, and $(V + E - V_c)$ is a function of the probability of ionisation. Therefore as V, the electron accelerating voltage, is increased, more electrons are effective in ionisation. If the probability of ionisation is a linear function of the excess energy:

$$I(V) = k(V + E_m - V_c) \int_E^\infty n(E)dE$$ where E_m is the mean thermal energy of the electrons effective in ionisation, and, since the probability of ionisation is small at the point of first appearance, it is approximately true to write:

$$V_c = V + E_m$$

Thus if E_m is the same for the unknown (I) and the standard (2) then the difference between the two A.P.s may be obtained by looking at $V_1 - V_2$ i.e. the points of initial detectability. However, E_m is only the same when the probability for ionisation is the same; this may be approximated to empirically, by admitting the gases in the correct proportions. There is evidence to suggest that the ionisation probability is not a linear function of the excess energy[36], but the above is still a valid approximation.

In the extrapolated voltage difference method[32], the linear portions of the ionisation efficiency curves are made parallel and the differences in electron volts, ΔV, corresponding to various values of ion current, I, are measured, and the graph of ΔV versus I plotted and extrapolated to zero ion current. The extrapolated value of ΔV is taken as the difference between the I.P. of the

standard and the A.P. of the ion under investigation. Although there seems to be little physical significance for this treatment, it is a method that has been widely used yielding results at least as good as those by other methods.

The logarithmic methods, based on Honig's[33] method, arise from a consideration of the energy spread of the electron beam emitted by the filament. In Honig's method the energy spread is accounted for by an analytical expression that describes the ionisation efficiency curve near the threshold. A semi-logarithmic plot reflects the linear shape of the original curve and the A.P. is obtained from the position on the curve where the slope = $2/3kT$, (k = Boltzmann's constant and T = the absolute temperature), from Honig's expression which considers the probability of ionisation as being equal to the square of the excess energy above the threshold. This method is said to be more accurate[37,38] than the straightforward linear extrapolation procedure mentioned earlier.

Lossing et al[39] used a simple modification of Honig's method, whereby the logarithm of the ion current is plotted as the percentage of the ion current at 50 ev, and the difference between the I.P. of the standard and the A.P. of the unknown taken at the arbitrary point of I% of the peak height at 50 ev. In this method the two ionisation efficiency curves must have the same shape and the peak heights of the respective ions must be normalised i.e. their ion currents made equal at 50 ev.

For completeness, a method introduced by Morrison[40] will be

mentioned here. In this, by considering the second derivative of the ionisation efficiency curves, he aimed at showing the presence of structure on the curves due to the formation of ions in excited states.

Summary

The established methods of interpreting ionisation efficiency curves stem from some form of treatment of the linear portion of the curve or from taking the A.P. at the point where the ion current is first detectable. We decided that the latter was more readily justifiable, and scientifically sound, and so decided to develop a method based on that principle and in which, using high sensitivity, we would concentrate on the region around the threshold.

Errors

The errors involved in any determination of A.P. will obviously depend on the manner in which the ionisation efficiency curves are interpreted, and will in the main be factors which affect the area of initial onset.

The principal error here lies in the inhomogeneity of the electron beam energy, and is the main cause of the tailing in the ionisation efficiency curves (an additional cause being the close proximity of states with energy similar to that of the ground state). This energy spread is Maxwellian in nature and is due to the electrons being emitted from the filament with thermal energy, which Honig[33] expressed as:

$$dN(U) = (4\ mA/h^3)U\exp\ -\left[(Q + U)/kT\ \right]dU$$

where:

dN(U) = the no. of electrons of energy between U and U + dU emitted per sec, U = thermal energy of the electrons and m = mass of the electrons.

h and k are respectively Planck's and Boltzmann's constants

A = surface area of the filament and Q its work function

T = absolute temperature of the filament

Thus for a filament temperature of 2500°K, where kT = 0.215 ev the thermal energy spread of the electrons will be 0.2 to 0.4 ev.[41]

Other errors arise from:[35]

1. Contact Potentials in the ion source.
2. Field penetration into the ionisation chamber.
3. Changes in filament temperature.

The contact potential, between the filament and the ionisation chamber, depends not only on the metals used (gold plating is used to reduce its effect), but also on the nature and degree of surface contamination and may alter by as much as Iv when a sample is admitted.

Ideally the ionisation chamber should be a field-free space, however, this cannot be achieved in practice as finite slits are required for the entry of the electrons and for the withdrawal of the ions, and a weak field is necessary to assist the flow of ions into the main accelerating field. Certain steps may be taken to minimise these effects; the trap and ionisation chamber should be

at the same potential, since the slit in front of the trap is relatively wide such that a potential to the trap could cause a considerable field, even in the centre of the ionisation chamber, which, of course, directly affects the energy of the ionising electrons.

In order to maintain sensitivity it is necessary to apply a small voltage between the repeller and the ionisation chamber. The motion of an electron, under the conditions to which the centre of the ionisation chamber approximates, has been studied[42], and the results show that the variation in the position of the beam and, therefore in its energy, is negligibly small. Consequently the effect of the repeller voltage, if kept constant, will be to give the electrons an additional increment of energy (which should disappear in the comparison of the two A.P.)

The ion accelerating field has a similar affect to the above, except that the electrons are retarded as they enter the chamber, an effect which is much smaller than that of the repeller, and which may be eliminated by using magnetic scanning, keeping the ion accelerating field constant.

If the temperature of the filament increases, the spread in thermal energy increases, more electrons of higher energy are available, and therefore the tailing of the ionisation efficiency curve is increased. Thus it is desirable that changes in filament current be kept as small as possible.

It is fairly easy to see that if the ionisation efficiency curves of the unknown and standard are measured simultaneously, so that each experiences very similar conditions, then many of these effects will cancel out. In this respect the choice of the standard is very important, for if it is well matched to the unknown, certain of these errors need not arise at all. For example, if there is a large difference in mass between the standard and the unknown, then their respective ions will be formed in different parts of the electron beam, due to the presence of a magnetic field in the source region, and thus it is possible that the ions will be accelerated to a different extent, an effect which will not cancel out in the difference step. Similarly, if there is a large difference in A.P. between the ions under comparison, then the electron accelerating volts will have to be varied to a greater extent than if the A.P. were close together and this will in turn produce a change in filament temperature during the experiment.

So the ideal conditions are:

1. Trap and ionisation chamber at the same potential, (or trap slightly +ve with respect to the chamber so as to maintain sensitivity); and similarly the repeller and ionisation chamber.
2. Magnetic scanning.
3. Small changes in filament temperature.
4. Small difference in mass between the standard and the ion under investigation; small difference between their A.P.s.
5. Ionisation efficiency curves measured simultaneously.

Even after all these conditions have been met, a reliable value of A.P. will only be obtained if the assumptions of the particular method used for interpreting the ionisation efficiency curves (e.g. similarity of shape), are realised.

Although many literature values of A.P. are given to two decimal places, this should not be taken as an indication of the absolute accuracy of the result, but more as an indication of the care taken in carrying out the relevant measurements.

Monoenergetic method

The methods discussed so far have all suffered in some way from the problem of the inhomogenity of the energy of the ionising electron beam. Fox et al[34] devised the retarding potential difference method in an attempt to reduce this effect. In their method, the electrons, after initial acceleration, encounter a retarding field, V_r, (see diag. 1.5) applied to grid 2, which removes the lower energy electrons and therefore ensures that the least energetic of those transmitted have, in fact, zero energy. The electrons then fall through an accurately known potential, V, applied between grids 2 and 3, following which they produce the positive ions in the cage area. A reduction of $\triangle V$ in the retarding potential results in an increase in the positive-ion current, caused by electrons of energy between V and $V - \triangle V$. Thus by varying V and recording, for each value of V, the difference in ion currents corresponding to retarding potentials of V_r and $V_r - \triangle V$, an ionisation efficiency curve is obtained which is essentially identical with that which would result

Diag. 1.5: Monoenergetic Method of Fox et al.

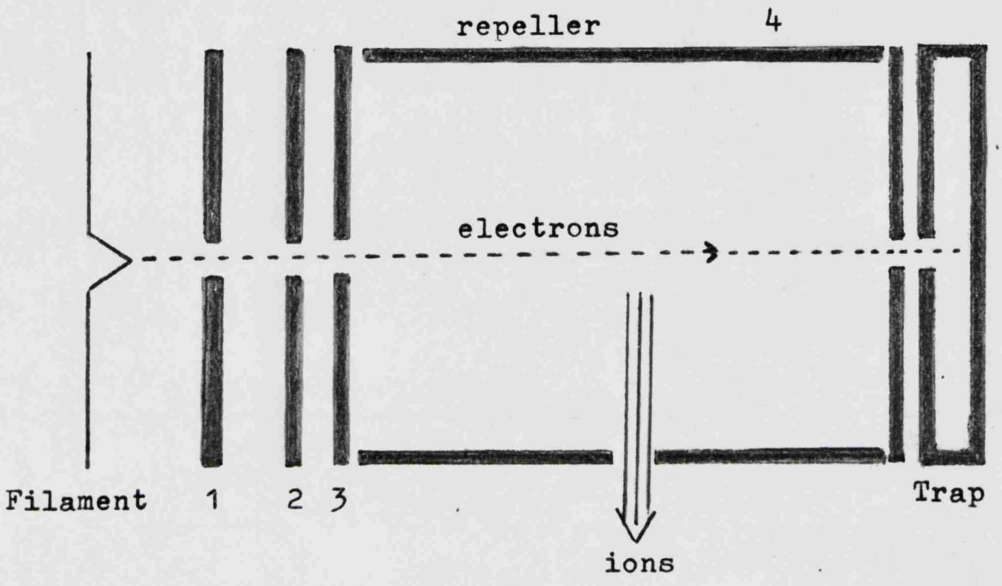

Retarding- Potential-Difference source.

from the use of a monoenergetic electron beam (see diag. 1.4).

The effect due to the repeller is tackled by pulsing: a negative pulse is applied to grid 2 after ionisation, supressing the electron beam and then a microsecond later a positive pulse is applied to grid 4 for the ion removal.

Using this technique, Fox has had considerable success in measuring A.P.s, and in elucidating fine structure on ionisation efficiency curves. However attempts to develop a commercially-available Fox-type source have been unsuccessful[43]. It was found to be practically impossible to obtain sound, reproducible results, because of the build up of space charges and field distortions, and the rectangular energy distribution of the electrons, as postulated by Fox, was only obtainable to a limited extent. Also, contact potentials built up very rapidly due to the contamination of the slits, and the trap was readily contaminated by the formation of an insulating spot at the point of electron impact.

Conclusion

The measurement of A.P.s, although by no means a fully-refined experimental technique, can, if adequate care is taken in choosing the experimental conditions, lead to reliable measurement of A.P., and if the A.P. has a value close to that of its adiabatic value (see diag. 1) a reliable value of bond dissociation energy can be deduced.

EXPERIMENTAL

Electron Impact Work

All measurements were carried out on an A.E.I. MS9 mass spectrometer which is based on the design of Nier and Johnson[44] incorporating electrostatic and magnetic sectors, both of 90° with r_e = 15 in. and r_H = 12 in., in the double focusing (second order) arrangement.

Method

The procedure was based on an idea of Gallagos and Klaver[45] in which the peak switching circuit of the mass spectrometer, by automatically switching the ion accelerating voltage at constant magnetic field, thereby enabling two peaks to be repeatedly displayed and recorded in turn, has been exploited for the measurement of ionisation efficiency curves. In carrying out the experiments the relevant peaks from the compound under investigation and a suitable standard were selected for display by the peak switching circuit and a signal sent by a relay in this circuit actuated a stepping motor attached to the potentiometer controlling the energy of the electron beam, so that after each complete cycle of the peak switching circuit the electron beam energy was reduced by a fixed small amount.

For this procedure, the helipot in the MS9 source supply chassis, which controls the energy of the electron beam, was replaced by an

equivalent low torque helipot (Beckman Instruments Ltd.), connected by a perspex shaft to the stepping motor (Impex Electrical Ltd., model A115055/80), mounted above the chassis. A 3:1 reduction gear was fitted to the motor so that each step reduced the electron beam energy by 0.05v. This step voltage was calculated by measuring the voltage change for a known number of steps with a sensitive, backed-off voltmeter at the ion source. The Measurement of the step voltage was carried out weekly since one would expect it to change as valves in the electron beam circuit of the mass spectrometer aged, however the variation over several months was very small.

The stepping motor circuit

With RLC, the relay in the peak switching circuit, as shown in the circuit diag., (diag. 2), C_2 was charged and when RLC switched C_2 discharged causing RL1 to close. When RLC switched again RL2 was closed momentarily by C_2 such that C_5 was connected across RL1, lowering its potential sufficiently for it to open. The necessary balance between relays RL1 and RL2 was achieved by adjustment of C_3. Relay RL3 was operated by an identical series of switchings and the whole sequence was indicated by the pilot lights LP1 and LP2.

The stepping motor

The motor consisted of a permanent magnetic rotor with twelve pairs of poles and two stators. The connections to the motor were made as indicated on the circuit diag. (diag. 2.0) such that step rotation was obtained by alternately reversing the direction of the fields flowing through the stators.

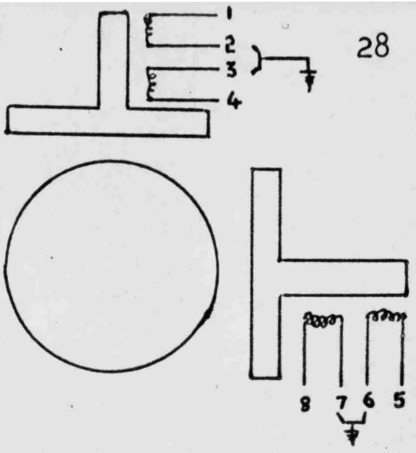

CONNECTIONS : STEPPING MOTOR

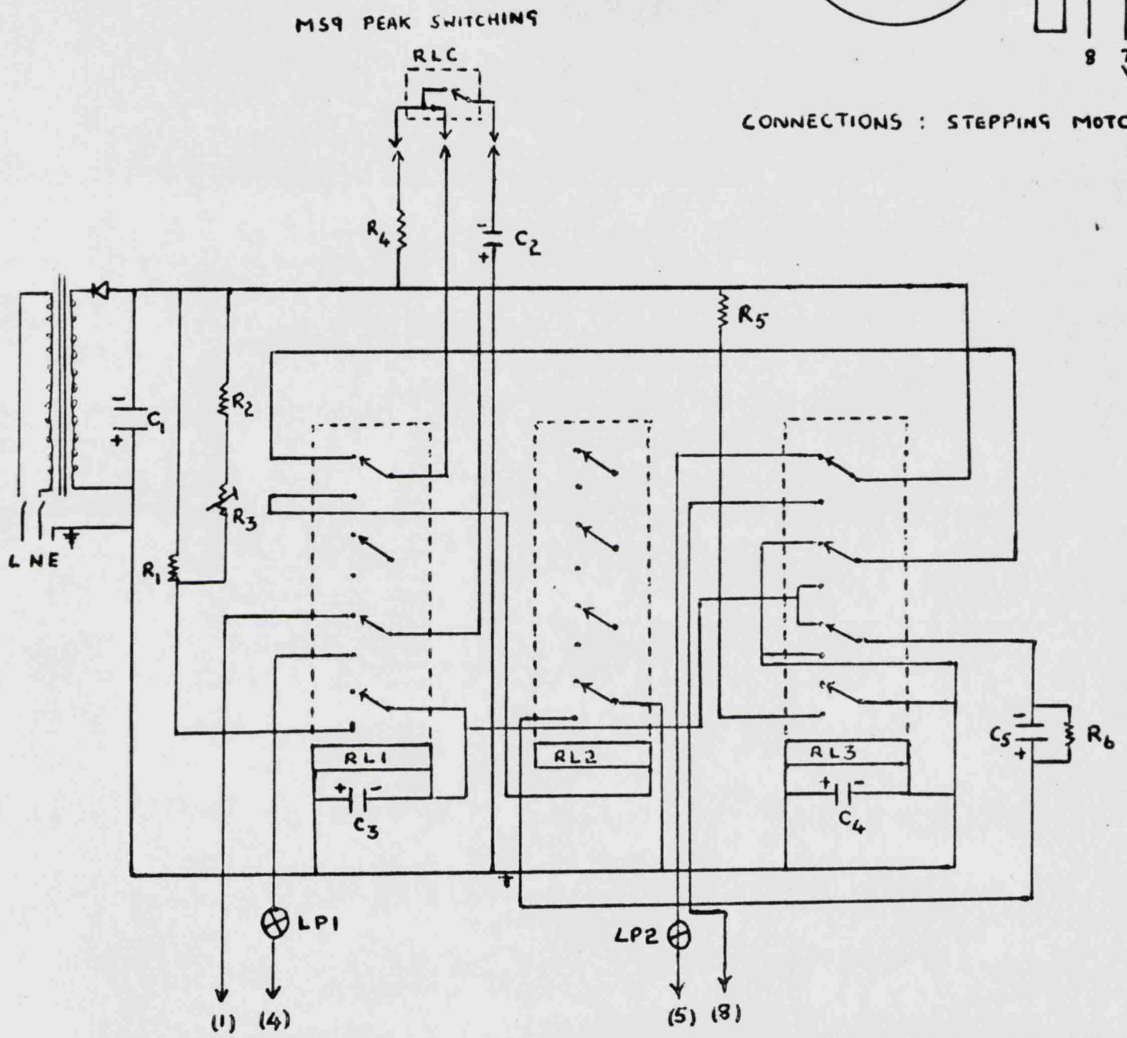

R_1	330 Ω	C_1	50V 3000μ
R_2	470 Ω	C_2	100μ
R_3	1K Ω	C_3	50μ
R_4	220 Ω	C_4	50μ
R_5	330 Ω	C_5	2000 μF
R_6	100 Ω		
LP1 LP2	3·5V; 0·15 A		
	REC 30		
	13V; 1·8 A		
$RL_{1,2,3}$	12V; 160 Ω		

Diag. 2.0: Stepping Motor Circuit.

Use of the method

The preliminary work was concerned with testing the method in order to find the best experimental conditions: experiments were carried out at various values of trap current and repeller voltage to ascertain how these would effect the A.P. measurements, and at the same time the results were analysed by the established methods, in order to find how these compared with our own method of interpretation. The conclusions were that the trap and repeller should be set at the same potential as the ionisation chamber, as in the well-tried methods[46], and that the methods of interpreting ionisation efficiency curves: the extrapolated voltage difference[32], vanishing current method[30], Lossing semi-log. plot[39], were no improvement on our own procedure (outlined below), far more tedious, and quite often unsuitable, since the assumptions implicit in their operation were often not valid.

In the first series of experiments the standards used were benzene and the noble gases, argon, krypton and xenon, and the particular standard for a certain measurement was admitted to the mass spectrometer, at the same time as the compound under investigation, through suitable inlets on the MS9. The procedure was modified in the work which yielded the final results[8,9,10]: the inlet used for the standards was one of the conventional ones of the MS9, the vapour being expanded into a 2 litre bulb, thereby giving a constant pressure throughout the experiment. The compounds under investigation were

admitted through an all-glass inlet which had been especially constructed for the halogen compounds studied in this laboratory[9,10]. The all-glass inlet, made by sealing a length of metrosil rod into a piece of glass tubing and then grinding the rod down to give a leak rate of 200 lusecs, was connected into the MS9 close to the ion source, thus giving a completely metal-free path.

Thus the results[8,9,10] were obtained by setting up the mass spectrometer with conditions so as to leave the ion source as 'field free' as possible: the trap current and ion repeller at cage potential; the electron multiplier was set so as to give maximum sensitivity. The source used in the experiments was one that was kept purely for A.P. work so that its condition was always clean and therefore free from contact potentials due to surface deposits. The compounds were then admitted to the mass spectrometer and the relevant peak from each displayed by the peak switching circuit. The peak heights were 'normalised' by adjustment of the sample pressures at 2v above the threshold, the stepping motor and recorder activated and the ionisation efficiency curves plotted simultaneously at 0.05v intervals.

The procedure had the following advantages:

1. It was a fully automatic method.
2. Maximum sensitivity was used.
3. The method was rapid.
4. Results were obtained simply, without plotting data.

1. The fact that the electron volts were decreased automatically meant that accurate and reproducible step size could be achieved, and that the operator was free to watch the overall conditions instead of concentrating on turning down the electron volts by hand. The use of the peak switching circuit in the automatic method enabled the curves of the sample and standard to be run simultaneously in a very convenient manner. (The advantages of obtaining the curves simultaneously was explained in the introduction.)

2. The use of maximum sensitivity is essential in any accurate measurement of A.P. that concentrates on the region around the threshold, since the ion current in that region is very low. Our method made use of the high sensitivity of the MS9 to gain a very accurate view of the points of initial detectability, and in fact amounted to a sensitive and direct extrapolation of the exponential part of the ionisation efficiency curves.

3. The attraction of a rapid method of determining A.P., apart from being less time consuming, is that the results can be obtained with the overall experimental conditions, particularly the electrostatic conditions in the ion source, being less likely to alter during the period of the experiment. The rapidity of our method was achieved because the stepping motor could be operated every 4 secs., with the ion currents being recorded immediately.

4. The difference between the A.P. of the standard and the ion from the compound under investigation, was read off directly from the

recorder trace (see diag. 2.1). Thus the method was far more convenient than the established methods, and it did not depend on any of the assumptions (similarity of shape etc.), implicit in their operation. Our method of interpreting the ionisation efficiency curves was therefore similar to the vanishing current or 'initial upward break' method, which has been criticised[35], mainly because results have been found to depend on the sample pressure. This point was investigated thoroughly, experiments being performed with sample pressures from 1×10^{-6} to 5×10^{-6} torr. Results were found to be unaffected by the changes in pressure. The reason for this may well be due to the high sensitivity of the MS9 and this would explain why the method was less successful for the measurement of an ion of very low abundance.

The drawback of our technique was that the ion accelerating voltage was altered by the peak switching circuit in bringing the sample and standard peaks into focus. This violates one of the fundamental conditions necessary for A.P. measurements, i.e. that the electrostatic conditions in the ion source should remain constant[47], however, Waldron and Wood[35] have shown that alteration of the ion accelerating voltage only affects the electrostatic conditions to a small extent. The actual magnitude of the effect for results determined in our apparatus was evaluated by applying the method to a series of compounds of known I.P.[48], see table 2. The size of the error, (the difference between the literature values of I.P. - the

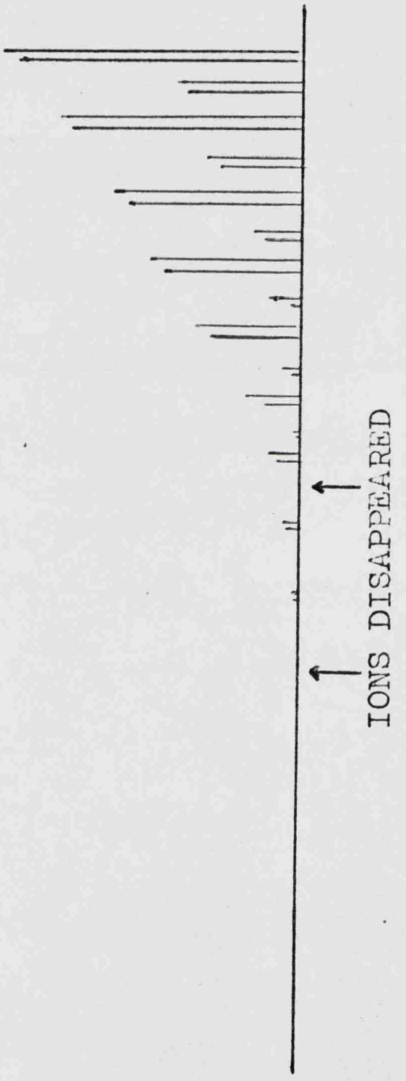

Diag. 2.I : Recorder Trace

COMPOUNDS	MASS RATIO	ΔI.P. LIT(ev)	ΔI.P. EXPT'L(ev)	ERROR(ev)
Xe, C_4H_9Br	1.046	2.0	1.85	0.15
Xe, $C_6H_5CH_3$	1.436	2.9	2.2	0.7
Xe, i-C_5H_{12}	1.573	1.5	1.3	0.2
i-C_5H_{12}, C_4H_9OH	1.028	0.3	0.21	0.1
i-C_5H_{12}, C_3H_7Cl	1.083	0.42	0.31	0.1
i-C_6H_{12}, n-C_6H_{14}	1.026	0.21	0.21	0.1
$C_6H_5CH_3$, CH_3Br	1.044	1.35	1.30	0.05
i-C_5H_{12}, Kr	1.166	4.4	2.2	2.2

$\Delta I.P._{LIT} = (I.P._X - I.P._Y)_{LIT}$

$\Delta I.P._{EXPT'L} = (I.P._X - I.P._Y)_{EXPT'L}$

ERROR $= \Delta I.P._{LIT} - \Delta I.P._{EXPT'L}$

Table 2: Application of the method to ions of known I.P.

STANDARD	MASS RATIO	ΔI.P. LIT(ev)	ΔI.P. EXPT'L(ev)	ERROR(ev)
i-C_5H_{12}	1.015	0.3	0.3	0
i-C_6H_{12}	1.150	0.6	0.65	0.25
Xe	1,81	1.2	1.9	0.7

Table 2.1: A.P. (Me_3Si^+) from Me_3SiCl, with various standards

difference found experimentally), can be readily seen from graph 2, which shows increasing error as the mass ratio, and hence the ion accelerating voltage, increases.

In the introduction, it was mentioned that errors can arise through differences in A.P. between the sample and standard. This effect[49] is common to all methods of determining A.P., and for our method the error produced by it is shown in graph 2.1, a plot of the error against difference between the literature I.P.s for the series of compounds in table 2. From the graphs it can be seen that in order to obtain results reliable to $\pm$ 0.1 ev, the sample and standard ions must have a mass ratio of less than 1.07, and a difference in A.P. of less than 1.3 ev; these conditions were adherred to throughout.

The usefulness of correlating the error with the choice of standard can be seen in table 2.1, which shows the results for the A.P. (Me_3Si^+) from Me_3SiCl, determined by other workers using the method[8]. The error in the result increases markedly with increasing mass ratio and $\Delta I.P._{LIT}$: from 0.0 ev with i-C_5H_{12}, to 0.7 ev with xenon as standard. The result with xenon also shows that the automatic choice of a noble gas as a reliable standard, as is done by many workers, may not necessarily be correct; the experimental technique and shape of the ionisation efficiency curve should be taken into account first of all.

The determinations of A.P. on Me_3SiX, X = Me_3Si, Me_2SiH, Me, H, were carried out at temperatures below 150° and each A.P. was measured at least 6 times.

Graph 2: Graph of Error against Mass Ratio

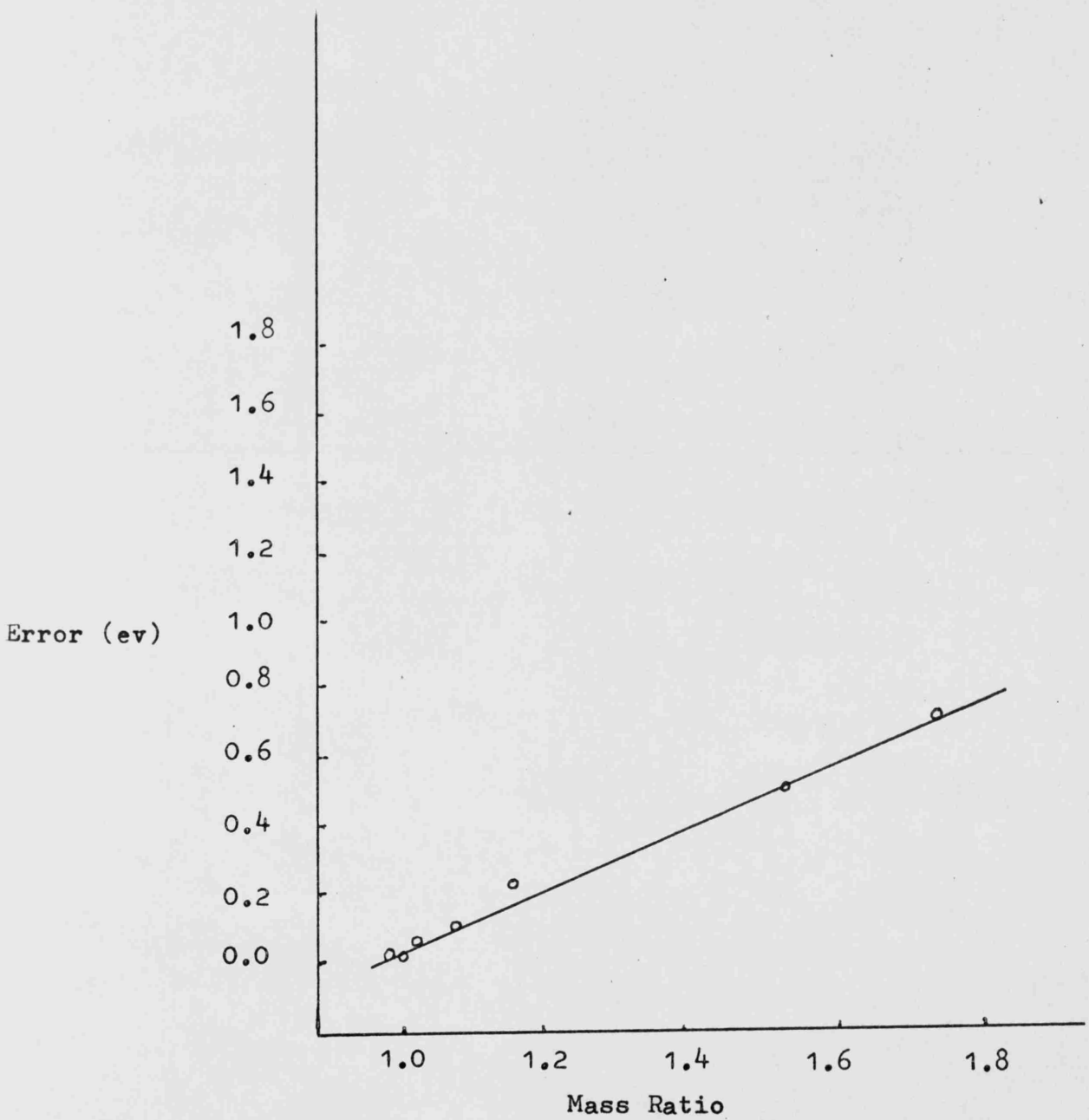

Graph 2.1: Graph of Error against Δ I.P.$_{LIT}$

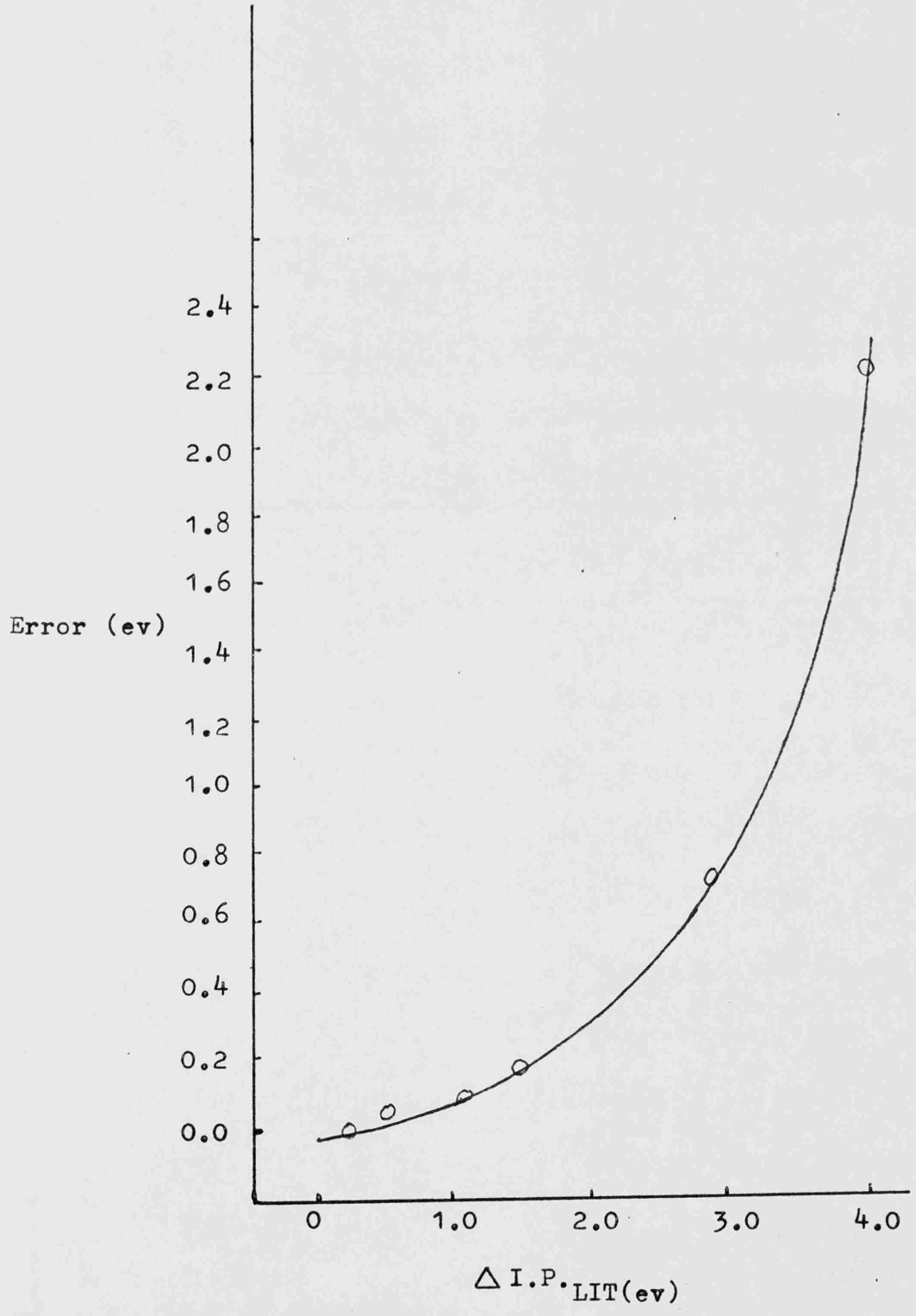

Kinetics

The kinetic experiments were carried out in a flow system centred about a stirred flow reactor connected into the mass spectrometer close to the ion source. The vacuum system is shown schematically in diag. 2.2.

The carrier gas, dry, oxygen-free nitrogen, admitted through tap, T_1, passed through the capillary, C_1, of known length and diameter, over the sloping manometer, M_1, and into two traps cooled by liquid nitrogen with between them a concertina of glass tubing the top half of which was heated to 200° while the bottom half was cooled in liquid nitrogen. The clean dry carrier gas now met the reactant flowing in from reservoir, R, through the needle valve, NV_2, entered the reactor, F, and exited through the product collection traps, and the magnetic valve, MV_1. This part of the system was entirely greaseless.

Sampling

The steady state products could be examined immediately and continuously by passing the furnace effluent gases through the leak, L_1, into the mass spectrometer, or, alternatively, larger amounts of product could be accumulated in the product collection traps, and then sampled by admittance to the mass spectrometer through L_1 or L_2. In this way accurate analysis of products from reactions of short contact time and small percentage decomposition could be readily achieved.

Diag. 2.2: The Flow System

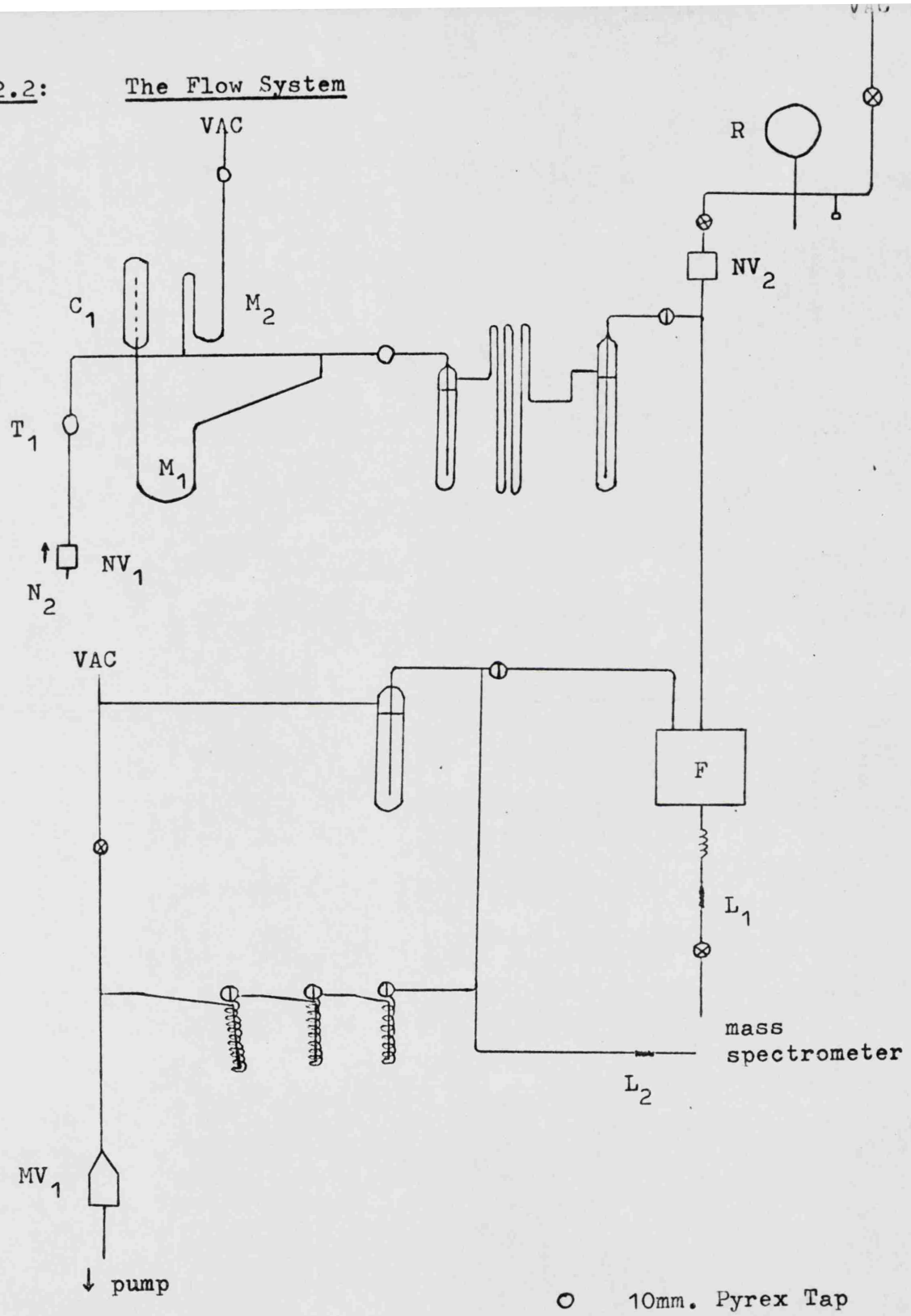

The reaction vessel

The stirred-flow reactor was based on a design of Mulcahy and Williams[50], and is shown in diag. 2.3. The vessel was a quartz sphere into which the gases were injected radially through the pinholes in the small sphere situated near the centre; the products exited tangentially through B, and the temperature was measured by a chromelalumel thermocouple placed in C (see below).

With a reactor of this design the reactants and carrier gas flow through the vessel continuously, and are mixed uniformly with the products so that when the steady state is reached, the effluent mixture has the same composition as the contents of the vessel. The method therefore substantially reduces the uncertainties regarding flow conditions and uniformity of temperature which are allied to conventional systems:

1. In a conventional system the gas is heated by thermal conduction as it flows through the reactor tube, the gas normally spending a substantial, but imprecisely known time, in the tube before it reaches the reaction temperature. In the stirred-flow system, however, the vigorous method of producing the mixing also brings about uniform temperature, and since the reaction occurs at the same rate everywhere in the reactor, no temperature inequalities are produced by the heat of reaction.

2. The conventional method assumes that no mixing of reagents and products occurs in the reaction tube, whereas, complete mixing is

Diag. 2.3: The Stirred-Flow Reactor

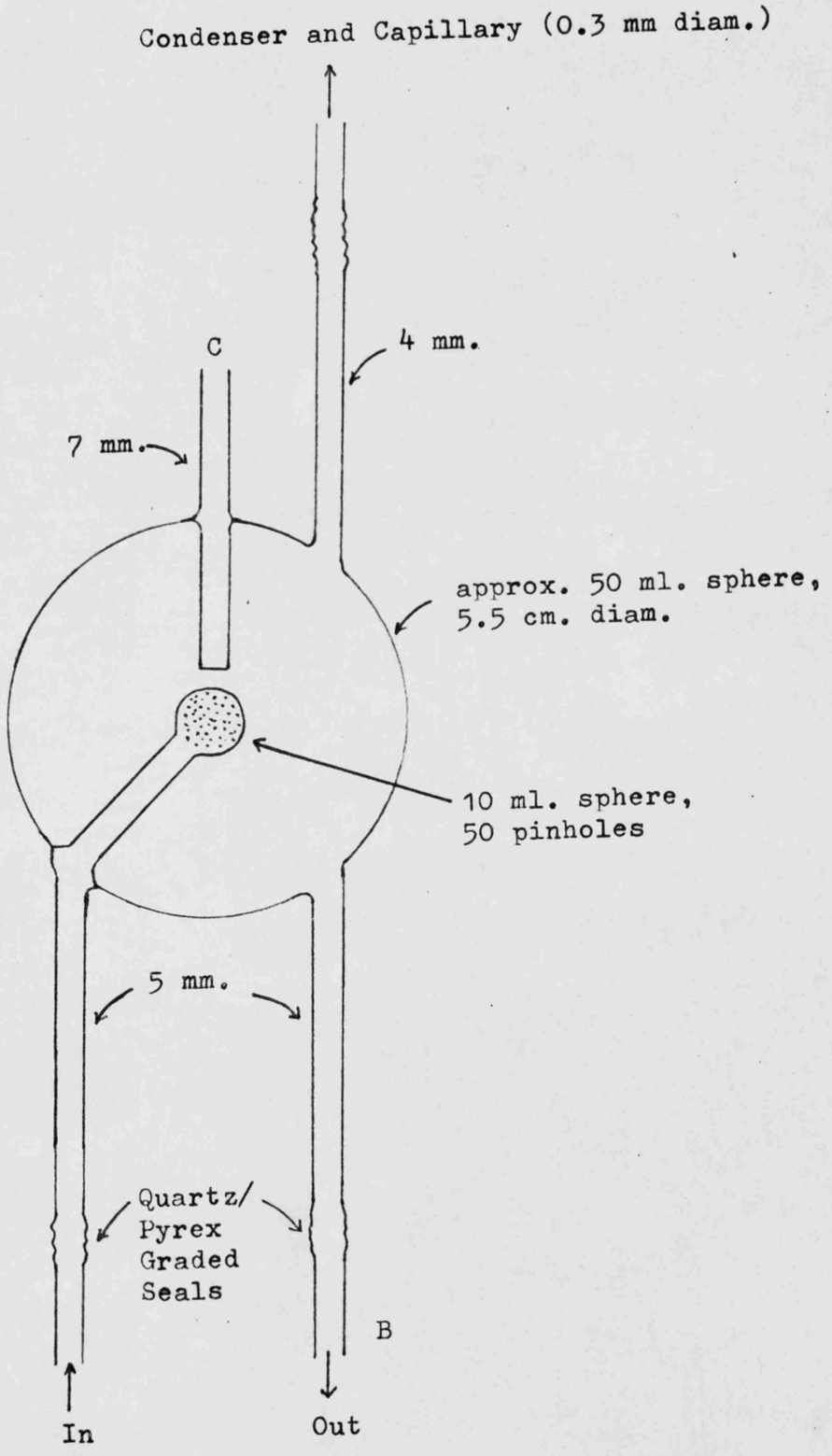

assumed in the stirred-flow reactor. The latter is a more realistic assumption since in any system there will always be a certain amount of mixing due to interpenetration by diffusion, and although this cannot be reduced it can be intensified, by a suitable device, as in the stirred-flow reactor. During the early work, before oxygen was completely eliminated from the system, low boiling point polymeric products were formed which tended to block the capillary of the reactor. The condenser, shown in diag. 2.4, was therefore constructed and fitted into the apparatus between the exit of the reactor and its capillary. The condenser was completely successful in preventing blockage of the capillary (once oxygen had been completely removed from the carrier gas, polymeric products were no longer formed in any case).

Seasoning of the reactor

The tendency of Si compounds to decompose heterogeneously on quartz surfaces is well known, as was exemplified by the conditioning found necessary for the pyrolysis of hexamethyldisilane[6]. Although the need for seasoning in a flow system should be reduced, it was thought worthwhile in this case, because of the heterogeneous behaviour experienced during the early stages of the work. The vessel was therefore subjected to repeated contact with the reactant, Me_3SiCl, and $SiCl_4$. It is difficult to say what good, if any, this achieved, since the heterogeneous behaviour was more than likely due to the trace amounts of oxygen within the system: when the sodium

Diag. 2.5:
Reservoir for Reactant

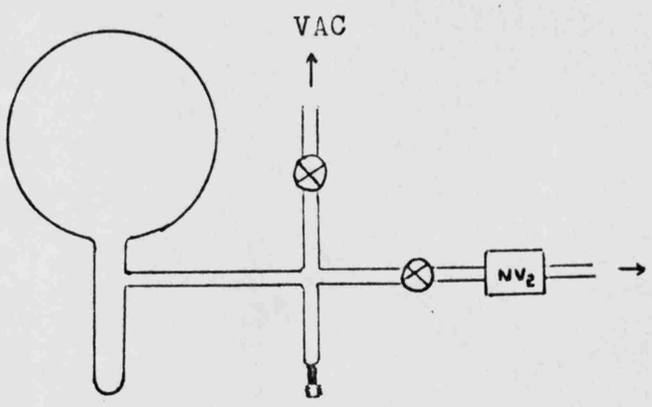

2 litre bulb

Springham Tap

Needle Valve

Adapter for filling reservoir

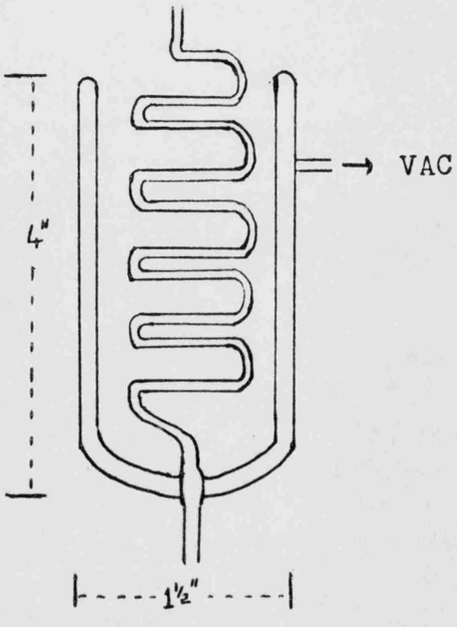

Diag. 2.4:
Condenser for Reactor

traps (see treatment of carrier gas) were fitted, and all the oxygen removed, homogeneous behaviour was rapidly achieved.

The Furnace

The furnace consisted of a stainless steel cylinder, (10" x 3"), coated with asbestos and wound with nichrome heating wire (4.7Ω per yard). The end plates were machined out of Sindanyo, to take the tubing of the vessel, which was located inside the furnace on a metal stool. A platinum resistance thermometer was fitted inside the furnace, directly underneath the vessel. The whole was well lagged with a 2" thickness of asbestos wadding and a uniform temperature was achieved over the complete length of the reactor by suitable tappings of the 5 heating windings. The conditions necessary for this were determined very readily by using a thermocouple as probe and viewing the temperature readings on a Solatron data logger.

The supply to the furnace was from a heavy-duty variac, and sensitive temperature control could be achieved by use of a Sunvic R.T.2. proportional controller and platinum resistance thermometer.

Temperature measurement

The temperature was measured by a chromel-alumel thermocouple and recorded by the data logger. The thermocouple was checked against a N.P.L. certified platinum/13° rhodium-platinum thermocouple and was accurate to $\pm$ 0.1°C.

Protection Devices

1. The diffusion pump heater was wired in series with the Flo Scan Alarm switch (G. A. Patton Ltd.) and the trip switch (see diag 2.8), such that the current supply was broken and the diffusion pump heater switched out if:

(a) the water flowing through the flo scan alarm was shut off, or it fell below the minimum level required to cool the pump.

(b) there was a power failure; the power was only restored to the diffusion pump heater when the trip switch was reactivated manually.

The rotary pumps also received their power via the trip switch.

2. The air admittance valves on the rotary pumps were each fitted with a 100 μF condenser so that their action was delayed by 5 sec., thus allowing the magnetic valves to close first, preventing air from entering the system.

The Pumping System

The flow was achieved by drawing the gases round the system with a rotary pump (Genevac), situated after MV_1, (Genevac), see diag. 2.2. Evacuation of the system was achieved in the conventional manner by use of a rotary pump and mercury diffusion pump. This part of the system also contained the Pirani and Penning gauge heads (Genevac types PGH1 and PNH1, respectively), and a by-pass for the diffusion pump to enable rough evacuation using only the rotary pump.

The pressure was read off a Pirani/Penning vacuum control box (Genevac type PP1), and experiments were only carried out at pressures below 5×10^{-4} torr.

Leak testing

Large leaks were found in the conventional manner by use of a tesla coil and for smaller leaks use was made of the MS9.

Flow Rate

The desired flow rate was achieved by using a suitable capillary, C_1, of known length and diameter, together with adjustment of the needle valve NV_1 (Edward's High Vacuum Equipment Model LB2B), at the inlet.

Using this principle a large range of flow rates could be achieved, giving contact times from 1 sec. to 1 min. The flow rate was evaluated from Poiseulle's eqn.[51]:

$$Q = \frac{10^3 d^4 (P_1^2 - P_2^2)\ 10^3}{0.68 L P_2} \qquad \text{ml.sec}^{-1}$$

where Q = flow rate

d = diam. of C_1, (inches)

L = length of C_1, (")

P_1, P_2, pressures either side of C_1, (torr). The pressures were obtained from the sloping manometer, M_1,$(P_1 - P_2)$, and from the manometer, M_2,(P_2). The manometers are shown on the schematic diag. of the system.

The contact time, or residence time, = V_r/Q, where V_r = vol. of reactor, (determined by weighing the reactor empty and full of water).

Treatment of the carrier gas

During the preliminary work the nitrogen carrier gas was dried by passing it through a column containing molecular sieve before it entered the flow system through polythene piping. Under these conditions it was not possible to obtain the carrier gas entirely free from oxygen, and so a new system was constructed out of copper so that better connections could be made between the nitrogen cylinder, drying column, and flow system. The device is shown in diag. 2.6. The latter method eliminated most of the oxygen which was entering by leakage, however the small amount of residual oxygen was still sufficient to cause the pyrolysis to be inhomogeneous and to give some siloxane products. The final traces of oxygen were removed by passing the nitrogen from the drying column through three traps containing sodium heated to 200°, see diag. 2.7. With these very vigorous conditions, no increase in the oxygen level over the background level of the MS9 was perceptible, and the kinetics immediately proceeded homogeneously, with no formation of siloxanes.

The reactant

Pure, dry trimethylsilane was vigorously degassed and stored in a 2 litre bulb with a cold finger attached, as shown in diag. 2.5. The purity and absence of oxygen were determined by mass spectrometry. A steady flow of trimethylsilane into the system, at the required concentration, was achieved by adjusting the needle valve (Edward's Ltd., Model LB13) and by keeping the cold finger in an ice bath.

Diag. 2.6:
Drying Column

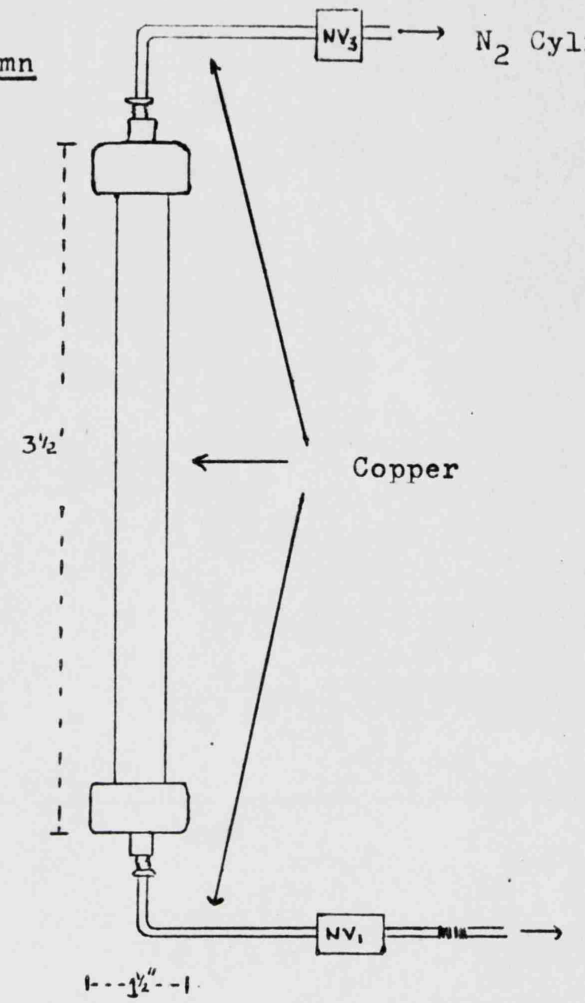

NV3 Needle Valve

NV1 Needle Valve

Glass to Metal Seal

Brass Screw Joins

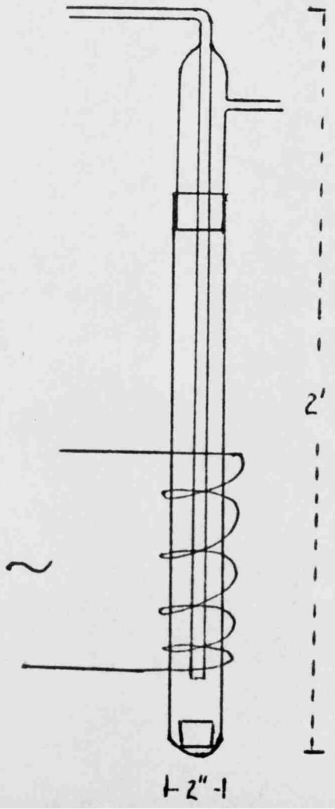

'Heat by the yard'

Nickel crucible containing sodium

Diag. 2.7: Sodium Trap

Diag. 2.9:
Split-Field Device

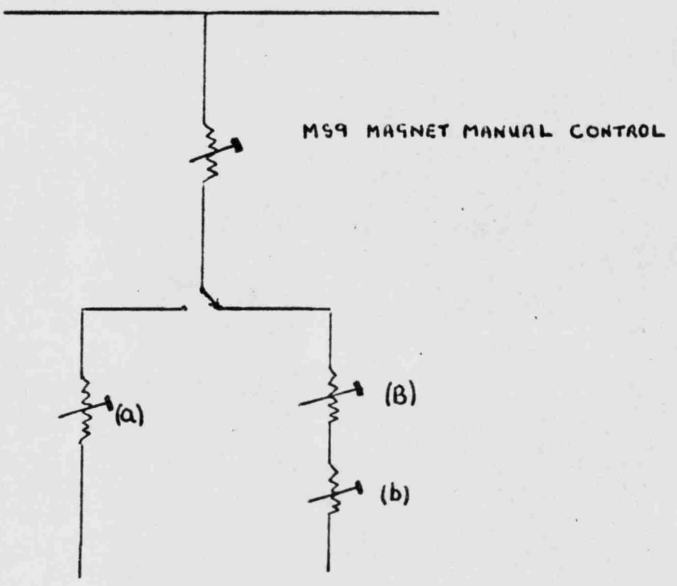

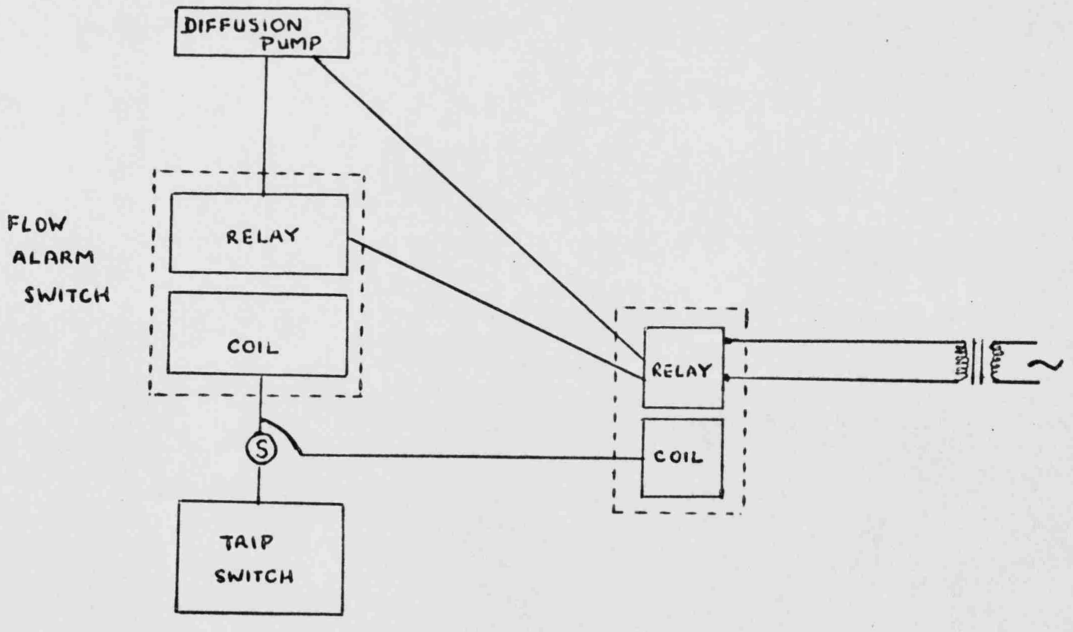

Diag. 2.8: Protection Circuit

The mass spectrometer split-field device

The magnetic scanning circuit of the MS9 was modified so that the magnet could be switched rapidly from one peak to another (see diag. 2.9). The 200Ω(a), 200Ω(b) and IK (B) potentiometers were connected in a series with the MS9 magnet coarse control through a double pole switch, so that the magnet could be focused in the relevant region with the MS9 coarse control and then focused on an ion of particular m/e with (a), the switch operated and another ion of given m/e focused on with (B), (coarse), and (b), (fine). Once the device was set up it was then just a matter of operating the switch to focus on each ion in turn. The method was readily adapted to the kinetic work, since it enabled the mass spectrometer to be switched rapidly between the reactant, and product peak of the pyrolysis. The base peak of trimethylsilane was taken as the concentration of reactant, i.e. Me_2SiH^+, m/e 59, and the product concentration was given by CH_4^+, m/e 16, the parent peak of methane, or H_2^+, m/e 2, the parent peak of hydrogen.

The use of the method

The system was set up with the carrier gas flowing round at the desired flow rate, and leaking into the mass spectrometer via the reactor. At the start of the experiment the background peaks for the reactant and product (either methane or hydrogen) were recorded using the split-field technique and data logger. The trimethylsilane

was allowed to flow into the system at a controlled rate of flow, and after steady conditions were achieved the furnace was allowed to cool slowly (5^{o} per minute) and the reactant and product peaks recorded together with the temperature.

The data logger was programmed to record a particular peak height nine times (one reading per second) followed by one reading of the temperature. Thus all the information necessary for an Arrhenius plot was obtained very rapidly, accurately and conveniently.

An example of the data recorded by the data logger is shown in table 2.2. All the readings down the extreme right hand side are of temperature (thermocouple reading x 40, for greater sensitivity); although only the temperatures corresponding to readings of reactant and product were required, the other temperature readings had to be recorded because of the logger programme. The other readings taken: background peaks, product and reactant peaks and range factor calibration (R.F.) are listed in the table.

The product peaks were measured on a different range of the MS9 to the reactant, and so a calibration reading was recorded for each run: a peak was measured on the range the product was measured on (X) and then on the range the reactant was measured on (Y) so that the reactant peaks were converted to the same scale as the product by multiplying by $\frac{Y}{X}$.

										Temperature
Background m/e 16		0065	0062	0077	0068	0075	0051	0067	0063	0065	+1180
Background m/e 59		0002	0002	0002	0003	0002	0003	0022	0002	0002	+1181
R.F.	X	0669	0655	0643	0643	0653	0656	0655	0669	0655	+1173
	Y	0014	0015	0014	0014	0014	0015	0014	0016	0014	+1175
(Methane)		1194	1138	1199	1211	1210	1212	1214	1208	1216	+1183
(Me_3SiH)		0721	0746	0751	0752	0748	0814	0779	0754	0696	+1186
(Methane)		1147	1139	1144	1141	1139	1133	1142	1136	1129	+1189
(Me_3SiH)		0810	0860	0865	0855	0801	0880	0845	0815	0784	+1194
		etc.									

where the concentration of reactant or product at a particular temperature is the average of the nine readings at that temperature

Table 2.2: Reactant = trimethylsilane, concentration given by Me_2SiH^+, m/e 59

Product = methane, m/e 16

At the end of the experiment the products which had been collected during a run were fractionated and their mass spectrum run.

The punch tape output of the data logger was fed into the computer (Elliot 803) and the Arrhenius parameters calculated.

Compounds: preparation and purification

Hexamethyldisilane, Me_6Si_2

Hexamethyldisilane was prepared by the method of Wilson and Smith[52] using the reaction:

$$2Me_3SiCl + \underset{\text{(alloy)}}{Na/K} \longrightarrow (Me_3Si)_2 + \underset{\text{(Na)}}{2KCl}$$

which was carried out under dry, oxygen-free nitrogen.

9.1g. sodium (0.4g. atom) and 63g. potassium (1.6g. atom) were cut into thin slices and placed in a three litre flask together with 400 ml. sodium-dried benzene. (The reaction would be more efficient if sodium and potassium wire were used, but the sheer bulk of the metal present makes this impractical.) 260 ml. (224g. 2.0 moles) of trimethylchlorosilane were added dropwise to the stirred mixture. After a while the solution turned purple and began to reflux gently. The solution was refluxed overnight, diluted with ethyl benzene and distilled over until the vapour temperature reached 130°. The remaining slurry was filtered into the distillate, through glass wool, and washed well with ethyl benzene.

The products were separated on a Vigreaux column, the refractive indices of the fractions measured and the samples collected when this property reached the desired value.

A 60% yield (approx. 1/2 mole) of hexamethyldisilane was obtained together with small fractions of trimethylchlorosilane and hexamethyldisiloxane.

The purity was ascertained by mass spectrometry:

b.p. 100.4°, n_D^{20} = 1.3772

The electron impact standards

Where possible analar reagents were used. If these were not available laboratory reagents were purified and used. The standards were all checked for purity by mass spectrometry.

Tetramethylsilane, Me_4Si

The tetramethylsilane was that used as an N.M.R. Standard (CIBA (A.R.L.) Ltd.), b.p. 27°, n_D^{20} 1.3588.

Trimethylsilane, Me_3SiH

The trimethylsilane was prepared by $LiAlH_4$ reduction of Me_3SiCl according to the eqn.:

$$LiAlH_4 + 4Me_3SiCl = 4Me_3SiH + LiCl + AlCl_3$$

and using 20 to 25% excess of $LiAlH_4$.

A slurry of 1.25g. (0.03 mole) lithium aluminium hydride in 150 ml. dry di-n-butyl ether was placed in a flask fitted with a dropping funnel, cold finger containing crushed ice, a stirrer, and an inlet through which dry, oxygen-free nitrogen was passed. 10.9g. (0.1 mole) commercial trimethylchlorosilane in an equal volume of the ether, was added to the slurry and the flask heated to maintain reflux.

The product, which was collected in a dry-ice-cooled trap, attached to the outlet of the cold finger, was transferred to a vacuum line and purified by trap to trap distillation using a CO_2 / acetone slush bath. The yield was 70% b.p. 7°, (lit. b.p.7°), and the purity was ascertained by mass spectrometry and G.l.c. Commercial trimethylsilane (Pierce Chem. Co. New York) was also used. It was purified as above.

Pentamethyldisilane, Me_5Si_2H

Pentamethyldisilane was prepared by a two stage process in

which pentamethylchlorodisilane, prepared in the first stage[53], was reduced[54] to give the desired product:

$$LiAlH_4 + 4Me_3Si_2Me_2Cl = 4Me_3Si_2Me_2H + LiCl + AlCl_3$$

8.0 ml. hexamethyldisilane and 12.0 ml. sulphuric acid (s.g. 1.84) were placed in a 100 ml. flask fitted with a stirrer, thermometer, and a cold finger, filled with crushed ice, attached to a system to collect the methane that was liberated. This consisted of an inverted gas jar, filled with water, over a bee-hive shelf. The reaction mixture was heated to 35° and stirred vigorously until no more gas was liberated. 700 ml. of gas were collected, (900 ml. calculated for), after 3 hours.

3.5g. dry ammonium chloride was then added over a period of 30 minutes and the mixture stirred for a further 45 minutes, whence the organic layer was separated yielding 8.0g. of pentamethylchlorodisilane.

8.0g. pentamethylchlorodisilane, (0.05 mole) in 20 ml. anhydrous ether, was added dropwise to 0.6g. (0.02 mole) lithium aluminium hydride in 50 ml. of ether. The mixture was heated gently under reflux during the addition in an atmosphere of dry, oxygen-free nitrogen, and after the addition heated for a further 12 hours to complete the reaction.

The product was separated from any solids by use of a Soxhlet apparatus, extracted with ether and fractionally distilled yielding 2.5 ml. of pentamethyldisilane, b.p. 97° (lit. b.p. 97°). The purity was verified by mass spectrometry.

RESULTS

Electron Impact

During the early work which was carried out to ascertain the best conditions necessary for the A.P. measurements, the noble gases were used as standards and the ionisation efficiency curves were interpreted by the well-tried methods[30,32,29] as well as by our own technique. Some examples of Lossing plots[39] are shown in diags. 3, 3.1. The results:

$$\left.\begin{aligned} \text{A.P. } (Me_3Si^+) &= 10.9 \text{ ev} \\ \text{A.P. } (Me_2SiH^+) &= 11.6 \text{ ev} \end{aligned}\right\} \text{ from } Me_3SiH$$

are higher than those obtained in the final experiments which is undoubtably due to the lack of experimental refinement at the time and to the differences in mass ratio and A.P. (see expt'l section), between the standards and ions under investigation. The Lossing method was modified slightly in that the standard and sample were normalised at 20 ev (instead of 50 ev) and the A.P. taken at 0% of the log. of the ion current at 20 ev, (instead of 1%).

The full set of results, obtained under the well established conditions as described in the experimental section, are shown in table 3.

Before any A.P. measurement was made the MS9 background was checked and if there was any doubt concerning the presence of a background peak in the m/e region under investigation a blank run

Diag. 3.: Me_2SiH^+ vs. Kr :

A.P.(Me_2SiH^+) = 11.6 ev

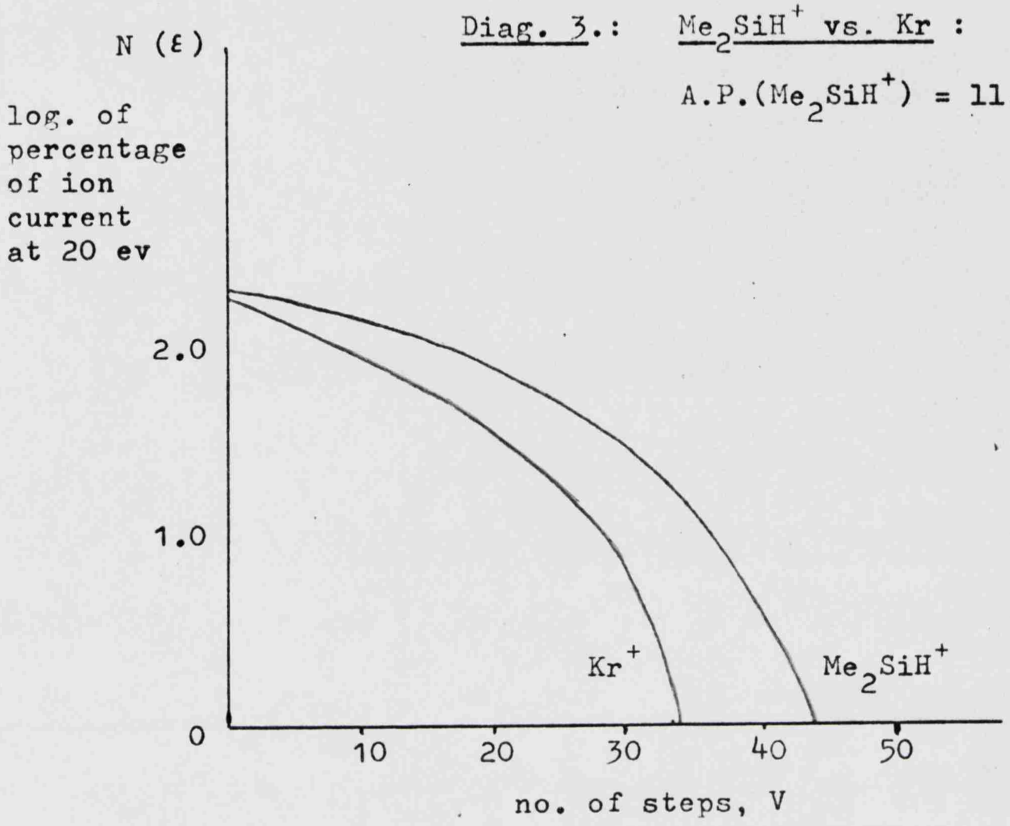

Diag. 3.1: Me_3Si^+ vs. Kr :

A.P. (Me_3Si^+) = 10.9 ev

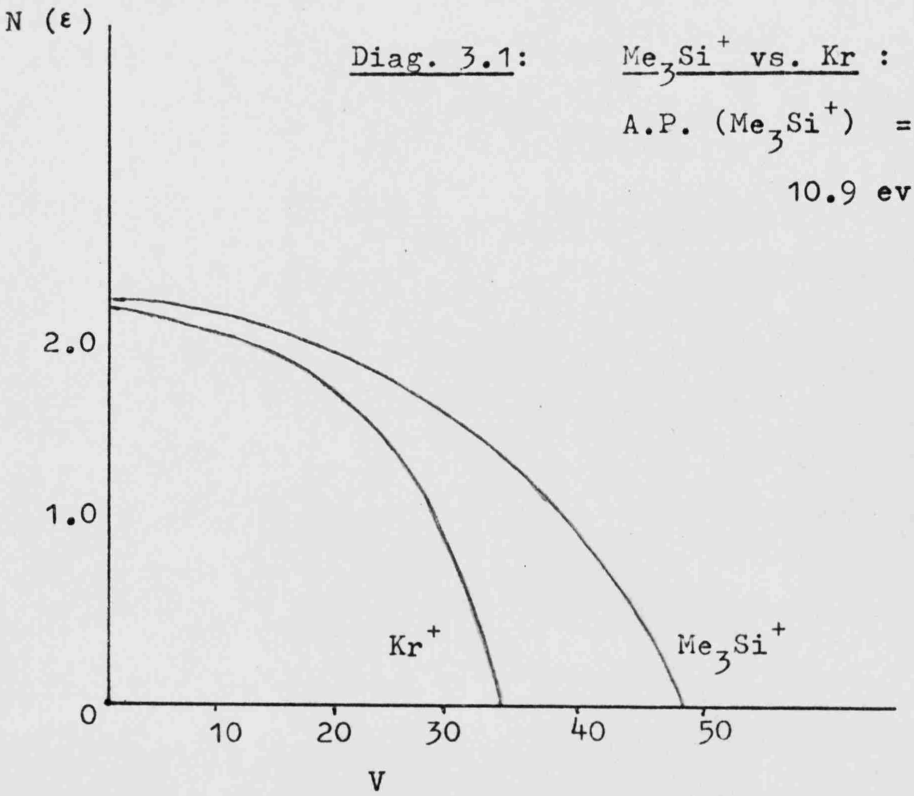

Diags 3,3.1: Lossing Plots for A.P. (Me_2SiH^+), A.P. (Me_3Si^+) from Me_3SiH.

COMPOUND	ION	STANDARD	A.P.(ev)
Me_6Si_2	Me_3Si^+	$i\text{-}C_5H_{12}^+$ *	10.0 ± 0.1
Me_5Si_2H	Me_3Si^+	$i\text{-}C_5H_{12}^+$	9.9 ± 0.1
	Me_2SiH^+	$i\text{-}C_5H_{12}$	10.7 ± 0.1
Me_4Si	Me_4Si^+	$i\text{-}C_6H_{12}^+$	9.9 ± 0.1
	Me_3Si^+	$i\text{-}C_5H_{12}^+$	10.4 ± 0.1
Me_3SiH	Me_3SiH^+	$i\text{-}C_5H_{12}^+$	9.6 (10.2)
	Me_2SiH^+	$i\text{-}C_5H_{12}^+$	10.6 ± 0.1
	Me_3Si^+	C_2H_5Cl	11.2 ± 0.1

* $n\text{-}C_3H_7Cl^+$ was also used with the same result

Table 3: Appearance Potential Measurements

COMPOUND	$D(Me_3Si - X)$ (kcal.mole^{-1})	$\Delta H_f^o(Me_3SiX)_g$ (kcal.mole^{-1})
$Me_3Si - SiMe_3$	67 ± 2	-118 ± 2
$Me_3Si - SiMe_2H$	65 ± 2	-103 ± 2
$Me_3Si - Me$	76 ± 2	- 68 ± 2
$Me_3Si - H$	81 ± 2	- 55 ± 2

Table 3.1: Bond Dissociation Energies and Heats of Formation

was performed. The mass spectrums of some of the compounds investigated are shown in diag. 3.2, where it can be seen that the compounds are characterised by the ion Me_3Si^+, m/e 73. The great abundance of the ion made it very amenable to investigation, and with the choice of i-C_5H_{12} as standard, (close in mass ratio and A.P.), enabled the results for A.P. (Me_3Si^+) to be confidently quoted to $\pm$0.1 ev.

Bond Dissociation energy

The bond dissociation energy, D(Me_3Si - X), may be calculated from:

$$\text{A.P. } (Me_3Si^+) = D(Me_3Si - X) + \text{I.P. } (Me_3Si.)$$

assuming excess energy is absent (conditions chosen to comply with Stevenson's rule[21]).

Since the I.P. ($Me_3Si.$) has not been determined by a direct method it must be calculated using the above eqn. with the A.P. (Me_3Si^+) from a compound of known D(Me_3Si - X). The calculations herein were based on the I.P. ($Me_3Si.$) determined using A.P. (Me_3Si^+) from Me_6Si_2, together with a kinetically determined value of D(Me_3Si-$SiMe_3$). Although there are several values of D(Me_3Si - $SiMe_3$) in the literature, the most reliable value was considered to be 67kcal.mole^{-1}.[6] The reasons for choosing this value are considered in the discussion.

Thus:

$$\text{I.P. } (Me_3Si.) = \text{A.P. } (Me_3Si^+)_{Me_6Si_2} - D(Me_3Si - SeMe_3)$$

$$= 10.0 - \frac{67}{23.06} \text{ ev}$$

$$= \underline{7.1 \text{ ev}}$$

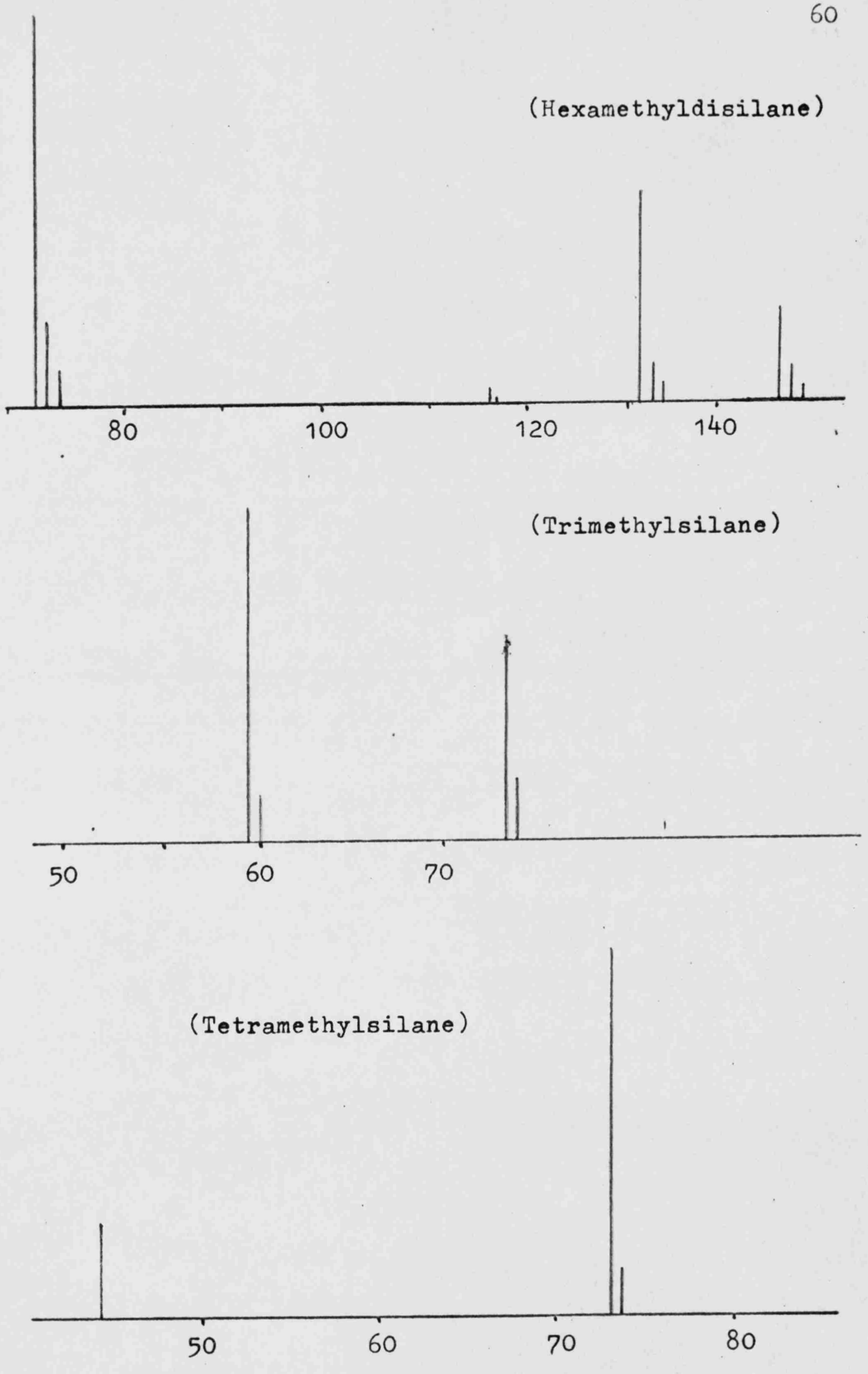

Diag. 3.2: Mass Spectra

Then combining the value of I.P. ($Me_3Si.$), with the values of A.P. (Me_3Si^+) from $Me_3Si - X$, the bond dissociation energies shown in table 3.1 were obtained.

Heats of formation

The heats of formation, $\Delta H_f^o(Me_3SiX)_g$, were calculated from the following equation:

$$\Delta H_f^o(Me_3SiX)_g = \Delta H_f^o(Me_3Si.)_g + \Delta H_f^o(X.)_g - D(Me_3Si - X)$$

Using the reliable recent literature value for $\Delta H_f^o(Me_3SiCl)_g$[55], together with the value of $D(Me_3Si - Cl)$ determined in this laboratory[10], the heat of formation of the trimethylsilyl radical was calculated:

$$\begin{aligned} \Delta H_f^o(Me_3Si.)_g &= D(Me_3Si - Cl) + \Delta H_f^o(Me_3SiCl)_g - \Delta H_f^o(Cl.)_g \\ &= 88 - 84.7 - 28.9 \\ &= \underline{-25.6 \pm 2 kcal.mole^{-1}} \end{aligned}$$

Then $\Delta H_f^o(Me_3Si.)_g$, together with $D(Me_3Si - X)$ and the heats of formation of the appropriate atoms and radicals[16], gave (using the above equation) the heats of formation shown in table 3.1.

Molecular and Radical Ionisation Potentials

The I.P. (Me_3SiX) is given directly from the A.P. (Me_3SiX^+). The intensity of the molecular ion was generally low and so the results are less accurate than those for A.P. (Me_3Si^+), and indeed, the result for I.P. (Me_3SiH) was ambiguous: 9.6 ev being obtained on several occasions whilst on others a value of 10.2 ev was obtained.

A value for the I.P. ($Me_2SiH.$) can be calculated using the value of $D(Me_2HSi - Me)$ from the pyrolysis of Me_3SiH (see discussion),

together with A.P. (Me_2SiH^+) from Me_3SiH:

$$\text{I.P.}(Me_2SiH\cdot) = \text{A.P.}(Me_2SiH^+) - D(Me_2HSi - Me)$$

$$= 11.2 - \frac{76.5}{23.06} \text{ ev}$$

$$= \underline{7.9 \text{ ev}}$$

The results are shown in table 3.2.

COMPOUND	I.P.
Me_3SiH	9.6
Me_4Si	9.9
$Me_2SiH\cdot$	7.9
$Me_3Si\cdot$	7.1

Table 3.2: Molecular and Radical I.P.

Kinetic Results

Before the work on trimethylsilane was started, the flow system was fully tested by pyrolysing di-t-butyl peroxide (DTBP), the kinetic parameters of which are well established. Experiments were carried out in the stirred-flow reactor at total pressures between 14 and 20 torr, and residence times between 0.5 and 3 sec. The kinetic parameters obtained were:

$$k = 0.11 \times 10^{16 \pm 1.0} \exp(-36100 \pm 1000/RT)$$

over the temperature range 500 to 520°K, with a maximum of 10% decomposition.

The only differences from the final system used for trimethylsilane was that the reactor was pyrex and that the method of recording the concentrations was by the conventional method of magnetic scanning on the MS9, the temperature being measured by a wheatstone bridge circuit.

Calculation of rate constant

The kinetics of the pyrolysis in a flow system have been considered in detail by Harris[56]. For complete mixing in the first order reaction:

$$A \xrightarrow{k_1} \text{product C}$$

$$Cc = \frac{Nc}{Ve}$$

$$Ca = \frac{Na}{Ve}$$

where Cc, Ca = concentrations of C and A respectively

Na, Nc = No. of moles of A, and C, respectively, leaving the reactor

Ve = effluent flow rate.

Also $Cc = t\,k,Ca$

and $t = \frac{Vr}{Ve}$

where Vr = vol. of reactor

$$k = \frac{Nc}{tNa} = \frac{Ve}{Vr}\frac{Nc}{Na}$$

And $Na = Nao - 1/n\ Nc$

$$Ve = Vo\left[\frac{Na + Nc}{Nao}\right] = Vo\left\{1 + \left[\frac{n - 1}{n}\right]\frac{Nc}{Nao}\right\}$$

where:

Vo = flow rate entering reactor

Nao = No. of moles of A entering reactor

n = No. of moles of product formed from 1 mole of reactant.

$$k = \frac{Vo}{Vr} \cdot \frac{Nc}{Na} \left\{ 1 + \left[\frac{n - 1}{n} \right] \frac{Nc}{Nao} \right\}$$

If n = 1 or if a large excess of carrier gas is present, i.e. no volume change

$$k = \frac{Vo}{Vr} \frac{Nc}{Na}$$

Thus in the pyrolysis of DTBP the rate constant, k, of the first order decomposition: $\left[(Me)_3CO\right]_2 \overset{k_1}{=} 2(Me)_2CO + C_2H_6$ was determined by measuring the rate of formation of acetone,

Na = $\left[(Me)_3CO\right]_2$

Nc = $(Me)_2CO$

Vr = volume of reactor = 100 ml.

Vo = flow rate.

The flow rate was obtained from readings taken from the sloping manometer, M_1, and the manometer M_2 (see diag. 2.2, expt'l section) using the Poiseulle equation[51].

The sloping manometer was calibrated using a cathatometer.

The reactant (DTBP) and product (acetone) concentrations were given by their peak heights (ion currents) as measured by the mass

spectrometer, i.e. m/e 146 and m/e 58 respectively. Two corrections had to be made in these measurements:

1. for the acetone formed from the breakdown of DTBP in the mass spectrometer.
2. for conversion of the peak height ratio into the molar ratio.

All the experiments were carried out with the MS9 ion source at 210°, therefore the correction for 1. was made by determining the mass spectrum of DTBP at 210°. The ratio of peak heights, DTBP: acetone was found to be 1 : 0.71 which meant that the concentration of acetone from the pyrolysis alone, was given by:

(peak height acetone) - 0.71 (peak height DTBP)

The molar ratio,2., acetone : DTBP, was determined by taking equal weights of the compounds by microsyringe and measuring the peak heights. It was found that the ratio was:

acetone : DTBP = 9 : 1

Thus for the peak heights measured during the pyrolysis to represent the molar concentrations of reactant and product:

$$Nc = 1/9\left[(\text{peak height acetone}) - 0.71\ (\text{peak height DTBP})\right]$$

$$Na = (\text{peak height DTBP})$$

The full kinetic results are shown in table 3.3 and examples of the Arrhenius plots, representing two extremes of contact time and total pressure are shown in diags. 3.3 and 3.4

Diags. 3.3, 3.4:

Arrhenius plots, log k(sec^{-1}) vs 1/T x 10^3 (^{o}K)

Diag. 3.3

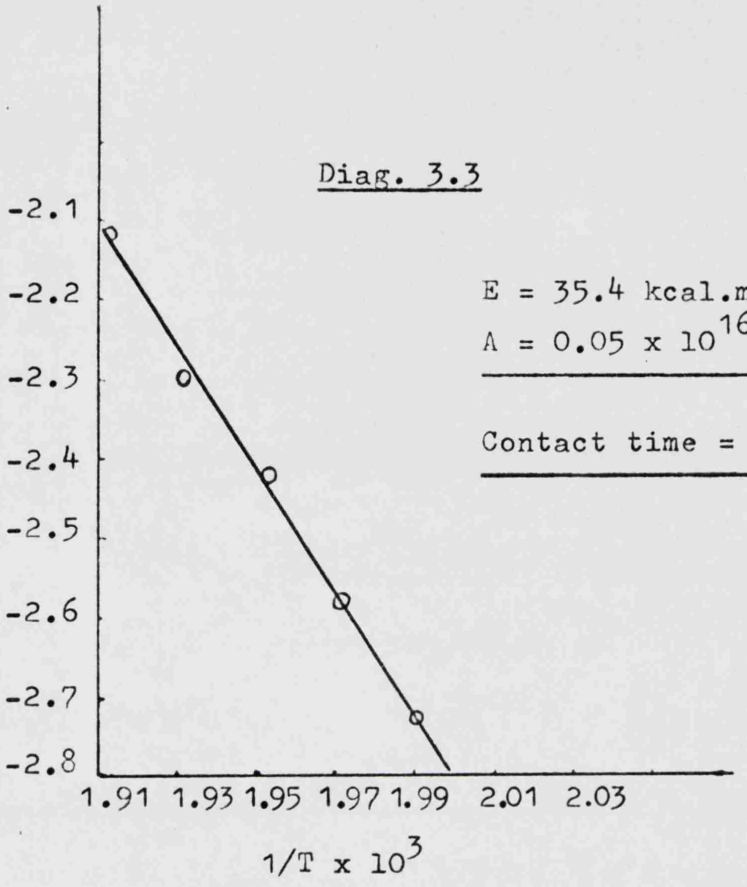

E = 35.4 kcal.mole^{-1}

A = 0.05 x 10^{16} sec^{-1}

Contact time = 0.5 sec

Diag. 3.4

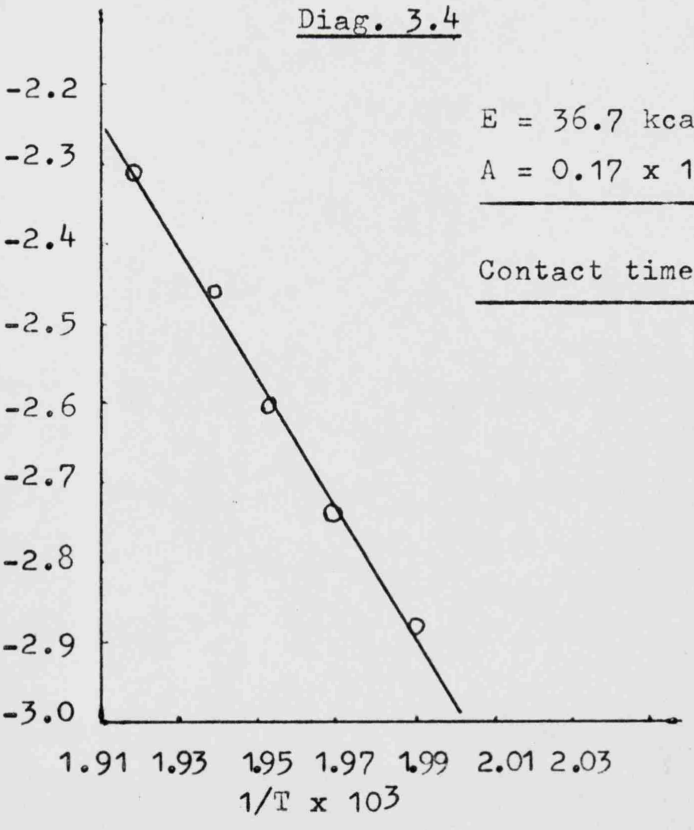

E = 36.7 kcal.mole^{-1}

A = 0.17 x 10^{16} sec^{-1}

Contact time = 3.0 sec.

Table 3.3: Full kinetic Results for Pyrolysis of DTBP

Run No.

(1) Vr = 100 ml.; Flow rate = 100.3 $ml.sec^{-1}$ (start); 89.3 $ml.sec^{-1}$ (finish).

Ratio of Peak Heights (corrected)	k	$T^{o}K$	log k	$1/T \times 10^{3}$
0.635	0.657	519.3	-0.1824	1.925
0.460	0.472	516.5	-0.3261	1.936
0.271	0.275	512.3	-0.5607	1.952
0.230	0.233	508.0	-0.6326	1.968
0.211	0.213	503.0	-0.6796	1.988
0.156	0.157	498.0	-0.8041	2.009
(2) Flow rate = 131.3 $ml.sec^{-1}$				
0.33	0.4467	519.3	-0.35	1.925
0.262	0.3533	517.5	-0.4518	1.932
0.172	0.2307	512.0	-0.6769	1.953
0.123	0.1647	508.3	-0.7833	1.967
0.103	0.1378	502.5	-0.8608	1.990
(3) Flow rate = 34.7 $ml.sec^{-1}$				
0.92	0.42	522.3	-0.3768	1.915
0.62	0.273	516.5	-0.5638	1.936
0.535	0.224	513.0	-0.6498	1.949
0.407	0.165	507.5	-0.7825	1.971
(4) Flow rate = 34.7 $ml.sec^{-1}$				
1.05	0.49	521.8	-0.3098	1.917
0.775	0.344	516.5	-0.4634	1.936
0.591	0.252	512.5	-0.5986	1.952
0.441	0.181	508.3	-0.7423	1.967
0.330	0.131	502.5	-0.8827	1.99

The pyrolysis of Trimethylsilane

From the electron impact results it was expected that the pyrolysis of trimethylsilane would proceed according to:

$$Me_3SiH \xrightarrow{k_1} Me. + Me_2SiH.$$

$$Me. + Me_3SiH \longrightarrow CH_4 + Me_3Si.$$

and similarly,

$$Me_3SiH \xrightarrow{k_{1'}} H. + Me_3Si.$$

$$H. + Me_3SiH \longrightarrow H_2 + Me_3Si.$$

Both stages would then be followed by radical combination to give an overall simple non-chain process; the rate of formation of methane would lead to the activation energy for the unimolecular dissociation with rate constant, k_1, and this would be equal to $D(Me - SiMe_2H)$. Similarly, by measuring the rate of formation of hydrogen, a value for $D(Me_3Si - H)$ would be obtained.

Using the method as described in the experimental section, the rates of formation of methane and hydrogen were measured and their respective rate constants evaluated as was shown for DTBP:

$$k = \frac{Vo}{Vr}\frac{Nc}{Na}$$

where Vo = flow rate, $ml.sec^{-1}$

Vr = volume of the reactor = 57.9 ml.

Nc = concentration of methane or hydrogen

Na = concentration of trimethylsilane

The necessary information for converting the peak height ratios into molar ratios was obtained by measuring the peak heights given

equal pressures of trimethylsilane, methane, and hydrogen. Several methods of measuring the pressure were used: McLeod gauge, mercury and di-n-butyl phthalate manometers, the measurements being read with a cathetometer. The results,

$$Me_3SiH : CH_4 = 2.9 : 1$$

$$Me_3SiH : H_2 = 3.7 : 1$$

are shown in table 3.6.

Thus for Nc, the product being methane:

$$Nc = 2.9 \times (\text{peak height of methane})$$

where the peak height is the average of nine readings recorded by the data logger, converted to the same scale as Me_3SiH by multiplying by the range factor calibration (see expt'l section).

Kinetic Parameters

The results were: from 670 to 758 C, 3to 50% decomposition, and total pressures 2 to 4 torr,

$$k_{CH_4}\ (sec^{-1}) = 10^{15.84 \pm 0.5}\ exp^{-76500 \pm 500/RT}$$

$$k_{H_2}\ (sec^{-1}) = 10^{15.99 \pm 0.5}\ exp^{-80300 \pm 500/RT}$$

Typical examples of some of the Arrhenius plots obtained are shown in diags. 3.6, 3.7, (methane formation), and 3.8, 3.9 (hydrogen formation), and the full kinetic results are shown in table 3.7 at the end of this section.

Order of reaction

The reactions were shown to be first order by the fact that there was no change in the rate constants with changes in reactant concentration of 50%.

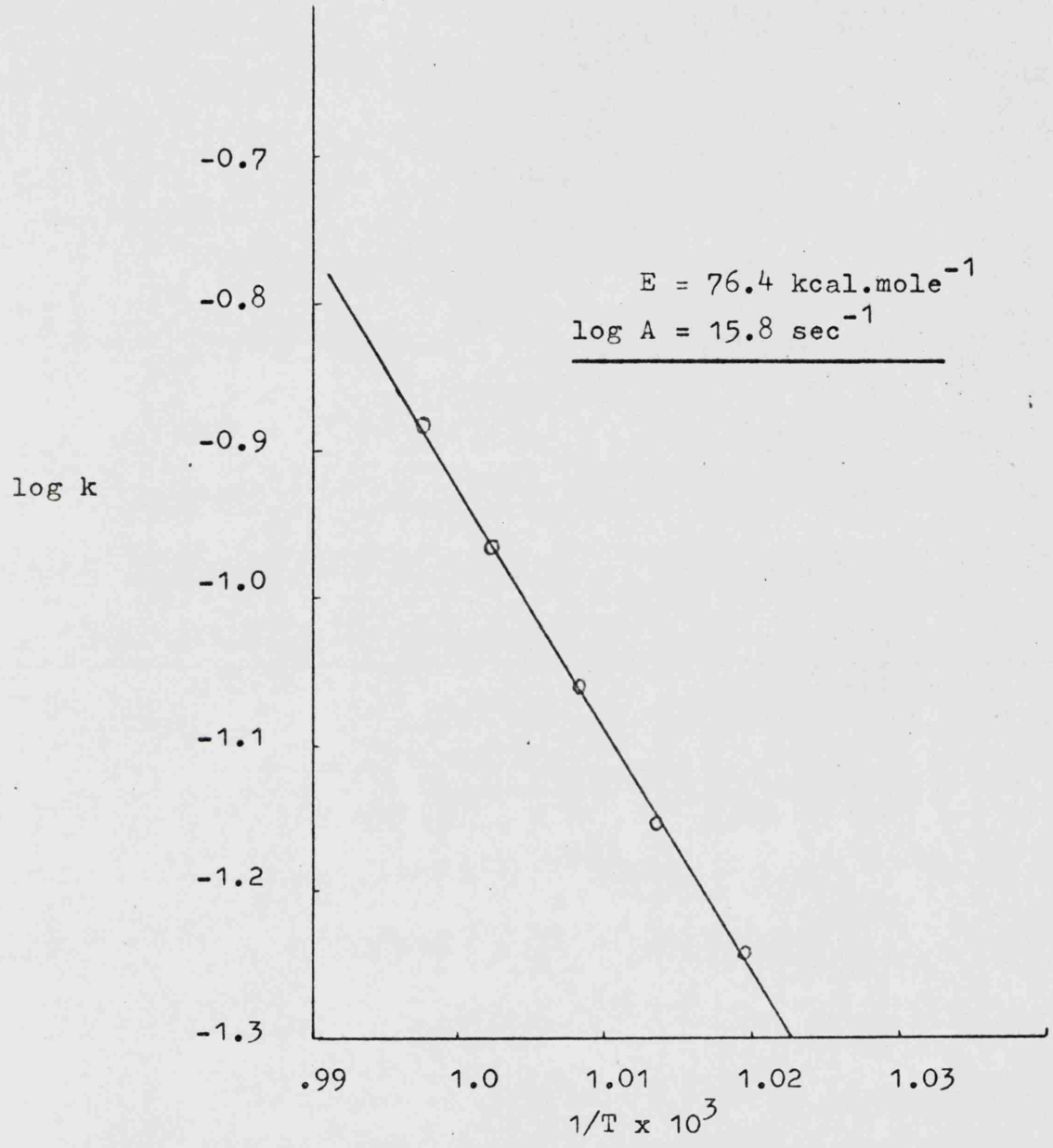

Diag. 3.6: Arrhenius Plot, logk (sec^{-1}) vs. 1/T x 10^3(^{o}K)

$^1/_t$ = 0.2976 sec

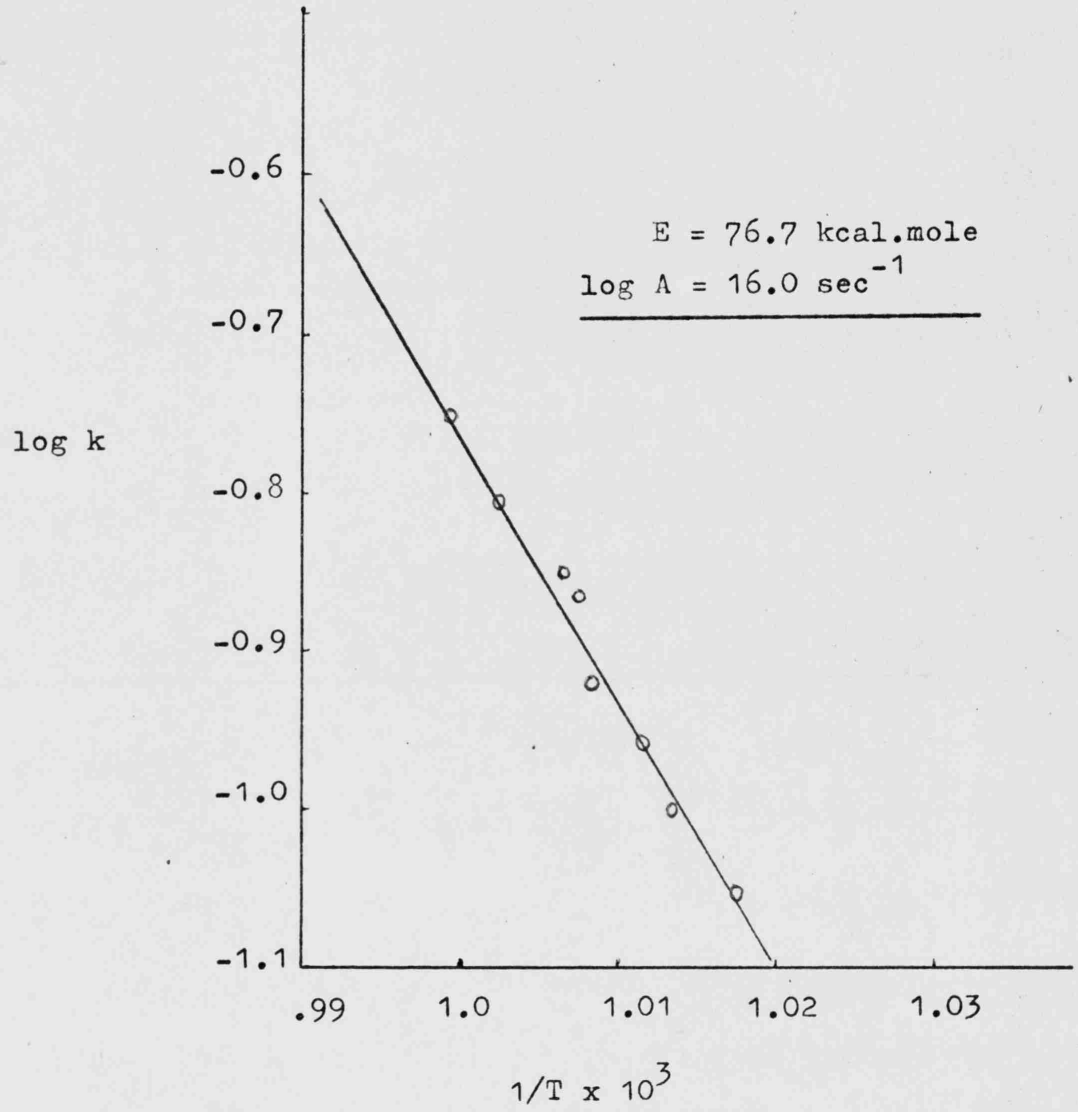

Diag. 3.7: Arrhenius Plot, log k (sec^{-1}) vs 1/T x 10^3(^{o}K)

$^1/_t$ = 0.2807 sec.

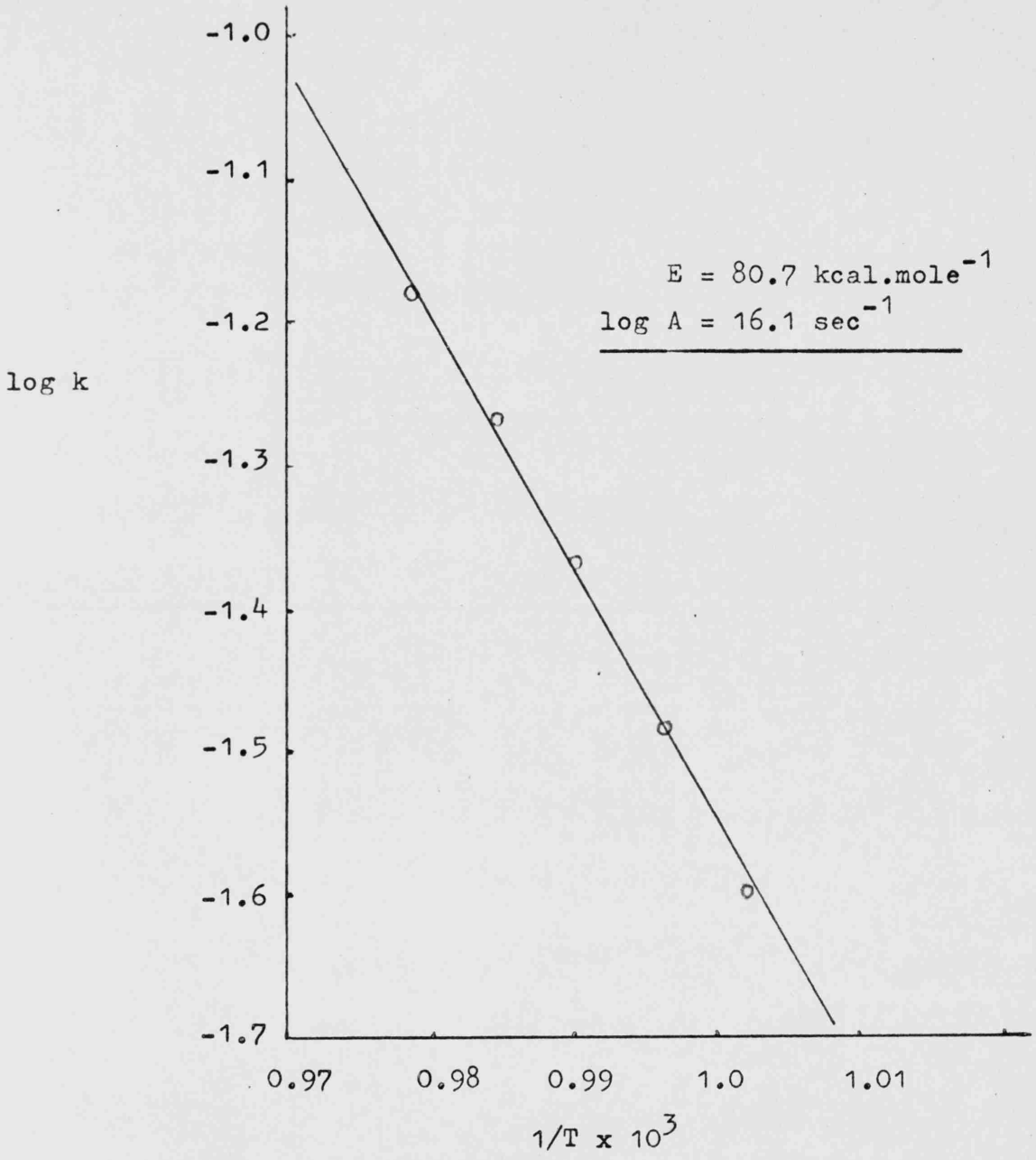

Diag. 3.8: Arrhenius Plot, log k(sec^{-1}) vs 1/T x 10^3(^{o}K)

$^{1}/_{k}$ = 0.2891 sec

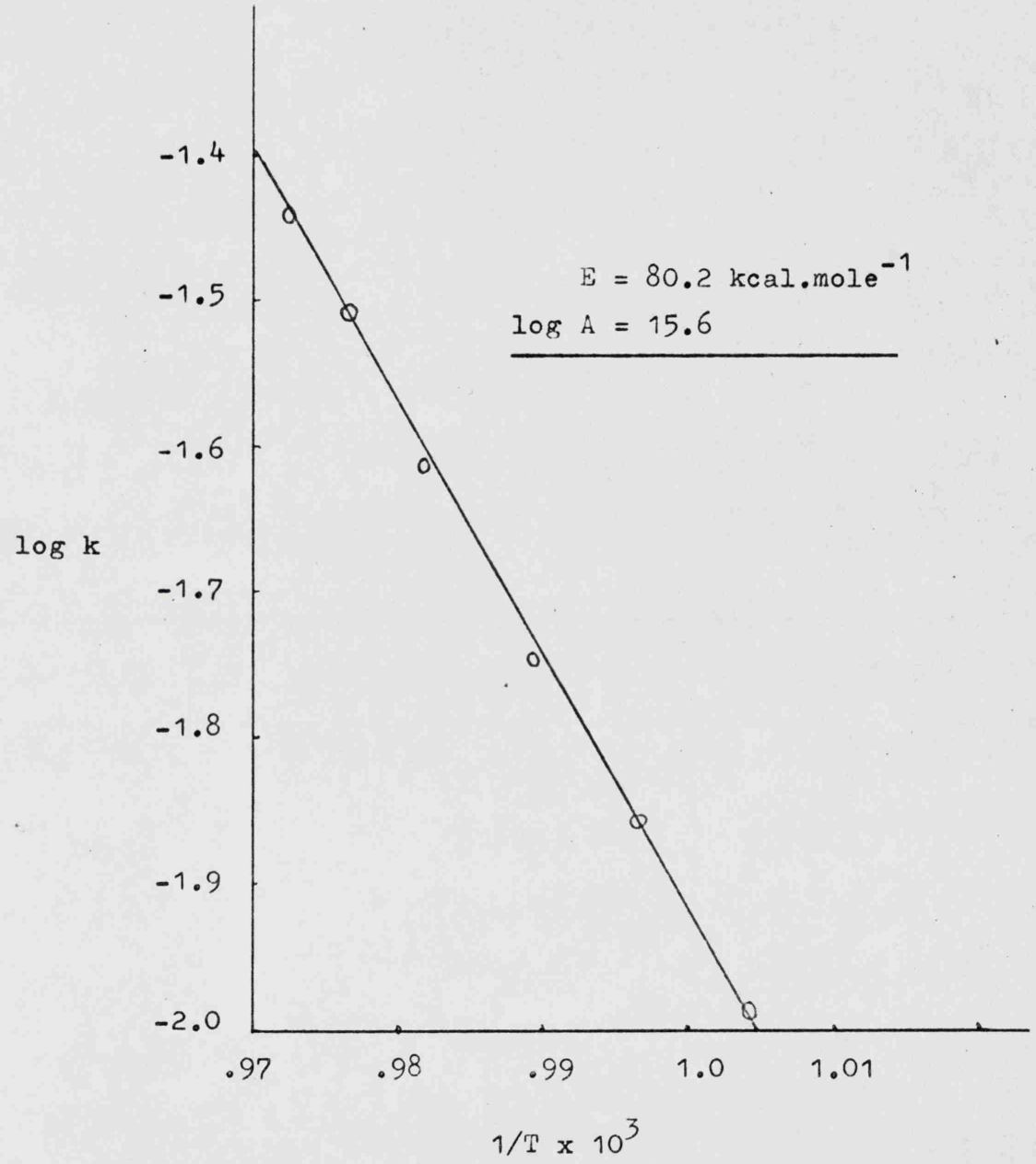

Diag. 3.9: Arrhenius Plot, log k (sec^{-1}) vs 1/T x 10^3(^oK)

$^1/_t$ = 0.2976 sec

Products

(i) Siloxanes

Organosilicon compounds generally react very readily with oxygen and moisture to form siloxanes; trimethylsilane was no exception so that elaborate precautions were necessary to eliminate oxygen from the flow system. In the initial stages of the work, when trace amounts of oxygen were still present, relatively large quantities of siloxanes were formed. These were given the probable structures I to IV; the prominent peaks from the mass spectra are shown in parenthesis:

$Me_3SiOSiMe_3$

I (147)

$Me_3SiOSiMe_2OSiMe_3$

II (221)

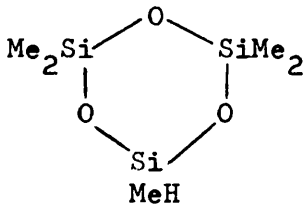

III (207,193)

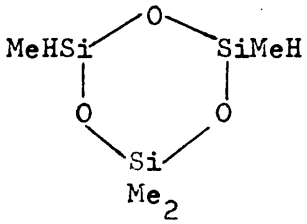

IV (193,179)

(ii) Pyrolysis products

During an experiment the products were collected in a liquid nitrogen trap and then separated from Me_3SiH at the end of the experiment by a trap to trap distillation, the products being retained by a CO_2/acetone slush bath. Samples of the collective products were admitted to the mass spectrometer through an all-glass

inlet, and the mass spectrum measured at a series of ionising electron energies. The mass spectra were interpreted from what was known in the literature[57], and by comparisons with the cracking patterns of organosilanes which were well-characterised from previous work done in this laboratory[7]. This procedure enabled the products to be identified as disilanes and disilamethylenes, disilacyclobutanes and very small amounts of dimethyl- and tetramethyl-silanes.

Disilanes and Disilamethylenes

It was very difficult to distinguish between the disilanes and disilamethylenes since, being isomers, they gave very similar cracking patterns. Both sets of compounds correspond to the peaks found in the spectra: weak parent peaks, strong fragments peaks at parent-methyl, parent-hydrogen and the characteristic Me_3Si^+, m/e 73, and Me_2SiH^+, m/e 59. The compounds are shown in table 3.4 where it can be seen that the disilamethylenes are distinguished by peaks corresponding to parent-hydrogen.

Compound	Mass	Main Peaks m/e
$HMe_2SiSiMe_2H$	118	118 117 103 59
$Me_3SiSiMe_3$	146	146 131 73
$Me_3SiSiMe_2H$	132	132 131 117 73 59
$Me_3SiCH_2SiHMe_2$	146	146 145 131 73
$HMe_2SiCH_2SiMe_2H$	132	132 131 130 117 73 59

Table 3.4: Disilanes and Disilamethylenes

Disilacyclobutanes

The product spectrum @ 70 ev was characterised by strong peaks at m/e 101; 115, 116; 130, 131; with weaker peaks at m/e 144 and 102. The ions with underlined m/e were the only ones remaining in the mass spectra measured at 6 ev, a strong indication that they were molecular ions. The alternative explanation viz. fragment ions was not supported since there were no parent ions visible above them, and in that m/e region the parent ions would have been quite strong: compare parent ions m/e 146 = 12%, m/e 204 = 42%, (where the strongest ion in the spectrum = 100%). The only explanation of the molecular ions was four-membered rings (there are no known compounds of silicon in three membered rings, and rings greater than four would not fit the observed m/e), the spectra corresponded to those given by disilacyclobutanes, and so the compounds were designated as shown in table 3.5

	Compound	Mass	Main Peaks m/e
(I)	Me_2Si  $SiMe_2$	144	144 129 101 64½
(II)	MeHSi 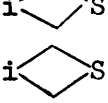 $SiMe_2$	130	130 129 115 57½
(III)	MeHSiSiMeH	116	116 115 101

Table 3.5: Disilacyclobutanes

The necessary information for interpreting the mass spectra came from what was known from Fritz's work[57] on (I), and the studies of Chernyak et al[58], on many alkylsilanes and silacycloalkanes,

which had established certain trends:

(i) silacycloalkanes were more stable than alkylsilanes and consequently gave much larger parent peaks than alkylsilanes of the same mass.

(ii) silacycloalkanes gave spectra very similar to the analogous hydrocarbons.

(iii) tertiary silicon atoms in silacycloalkanes were more stable than quaternary silicon.

Thus the trends would predict the order of magnitude of the parent peaks of (I), (II) and (III) as:

$$116 > 130 > 144$$

and parent-methyl peaks (relative to parent peaks) as

$$(P - Me)_{(I)} > (P - Me)_{(II)} > (P - Me)_{(III)}$$

where P - Me = parent-methyl peak

(I), (II), (III) = the compounds in table 3.6.

The predictions were fully met by the experimental results, and the mass spectrum of (I) was measured with the same results as found by Fritz[57].

Table 3.6

McLeod Gauge

Compound	m/e	Pressure (torr)	Peak height	Peak height at equal pressures	Ratio
Me_3SiH	59	0.05296	70.5	76.14	2.43
CH_4	16	0.05720	31.5	31.5	1
Me_3SiH	59	0.0145	14.04	14.04	2.34
CH_4	16	0.0145	8.0	8.0	1
Me_3SiH	59	0.03245	26	29.9	3.52
CH_4	16	0.0375	8.5	8.5	1

Me_3SiH : CH_4 = 2.76 : 1 (average)

Mercury Manometer (Pressure read by cathetometer)

1) Me_3SiH

Pressure (arbitrary units)	Peak height	Peak heights at equal pressures	Mean value peak height
0.33	49.25	149.2	
0.225	36	160	
0.252	44.5	176.6	161.9
0.247	46.55	188.5	
0.543	68.25	125.7	

2) Methane, CH_4

0.485	20	41.2	
0.373	18.25	48.9	
0.167	10.75	64.4	52.47
0.182	10.5	57.9	
0.315	16	50.8	

Me_3SiH : CH_4 = 3.1 : 1 (average)

Di-n-butyl phthalate (pressure read with cathetometer)
(Each peak height average of nine readings)

Compound	m/e	Pressure (arb. units)	Peak heights at equal pressures	Ratio
Me_3SiH	59	1.40	1927.9	2.9
CH_4	16	0.97	664.8	1
Me_3SiH	59	0.68	732.7	2.9
CH_4	16	0.68	252.7	1

Me_3SiH

Pressure	Peak height	Peak height at equal pressures	Average peak height at equal pressures
0.656	99.5	151.7	
0.485	83.5	172.2	167.9
0.410	64.0	156.1	
0.274	52.5	191.6	
Hydrogen			
0.23	9.75	42.4	
0.426	19.0	44.6	44.88
0.64	30.5	47.7	
0.677	30.3	44.8	

Ratio Me_3SiH : CH_4 = 3.7 : 1

Di-n-butyl phthalate

(Each peak height average of nine readings)

Me_3SiH

Pressure	Peak height	Peak height at equal pressures	Average peak height at equal pressures
0.2	41	205.0	
0.4	67	168.0	
0.6	93	155.0	169.5
0.8	120	150.0	

Hydrogen

0.2	8.2	41.0	
0.4	18.3	45.8	45.53
0.6	28.4	47.3	
0.8	38.4	48.0	

Ratio $Me_3SiH : H_2 = 3.7 : 1$

Conclusion: Molar Sensitivities $Me_3SiH : CH_4 = 2.9 : 1$

$Me_3SiH : H_2 = 3.7 : 1$

Table 3.7: Full Kinetic Results

Methane

Values of E ($kcal.mole^{-1}$)	Values of Log A	Run No.
76.3	15.9	1
76.4	15.8	2
76.4	15.6	3
76.7	16.0	4
76.4	15.8	5
76.4	16.0	6
76.9	16.0	7
76.9	15.8	8
76.8	15.8	9
75.8	15.6	10

Run No. (1)

1/t = 0.2807 sec

(Methane)=Nc (uncorrected)	$(Me_3SiH) = Na$	$k = \frac{1}{t}\frac{Nc}{Na}$ (sec^{-1})	log k	$10^3 \times 1/T(^oK)$
1008	1460	0.0566	-1.2472	1.033
1173	1371	0.07014	-1.1541	1.028
1452	1258	0.09462	-1.0240	1.019
1666	1134	0.1204	-0.9194	1.013
1861	1033	0.1477	-0.8306	1.009
2077	918	0.1854	-0.7319	1.003
2192	818	0.2196	-0.6584	1.000

Run No. (2)

1/t = 0.2976 sec

1024	1620	0.05653	-1.2478	1.019
1205	1544	0.06978	-1.563	1.013
1393	1443	0.08633	-1.0638	1.008
1619	1335	0.1076	-0.9681	1.002
1821	1242	0.1371	-0.8824	1.000

(Methane)	(Me_3SiH)	$k(sec^{-1})$	log k	$10^3 \times 1/T(^oK)$
Run No. (3)				
1/t = 0.2976 sec				
783	813	0.04156	-1.3814	1.018
935	754	0.05351	-1.2715	1.011
1047	678	0.06664	-1.1762	1.005
1193	597	0.08623	-1.0643	0.9982
1333	524	0.1098	-0.9593	0.9927
Run No. (4)				
1/t = 0.2807 sec				
1406	1309	0.08805	-1.0553	1.017
1549	1280	0.09923	-1.0034	1.013
1647	1234	0.1094	-0.9609	1.011
1749	1197	0.1198	-0.9215	1.008
1831	1103	0.1360	-0.8665	1.007
1896	1112	0.1397	-0.8547	1.006
2063	1081	0.1564	-0.8058	1.002
2143	998	0.1765	-0.7533	0.9991
2243	924	0.1991	-0.7009	0.9965
Run No. (5)				
1/t = 0.2976 sec				
744	1515	0.04251	-1.3715	1.028
913	1417	0.05576	-1.2536	1.018
1082	1304	0.07181	-1.1438	1.01
1220	1178	0.08962	-1.0476	1.004
1409	1046	0.1166	-0.9332	0.9973
1516	938	0.1399	-0.8541	0.9936

Run No.(6)

1/t = 0.2807 sec

(Methane) (uncorrected)	(Me_3SiH)	$k(sec^{-1})$	log k	10^3 x 1/T(°K)
817	1231	0.05441	-1.2643	1.030
943	1166	0.06631	-1.1784	1.024
1102	1074	0.08410	-1.0752	1.018
1222	997	0.1005	-0.9979	1.013
1331	923	0.1182	-0.9273	1.009
1419	873	0.1333	-0.8751	1.006
1556	784	0.1627	-0.7887	1.002
1613	753	0.1756	-0.7555	0.9982

Run No.(7)

1/t = 0.2807 sec

882	1306	0.07536	-1.2568	1.029
1059	1244	0.06978	-1.1563	1.021
1243	1145	0.08900	-1.0506	1.015
1456	1020	0.1170	-0.9319	1.008
1636	932	0.1439	-0.8420	1.003
1762	857	0.1685	-1.7734	0.9991
1961	771	0.2085	-0.6808	0.9955
2069	704	0.2410	-0.6180	0.9918
2149	641	0.2749	-0.5608	0.9883

Run No.(8)

1/t = 0.2421 sec

957	1784	0.01016	-1.9932	1.062
1361	1756	0.01467	-1.8335	1.052
1795	1707	0.01991	-1.7009	1.043

Run No.(9)

1/t = 0.2421 sec

1050	1683	0.01181	-1.9277	1.059
1449	1622	0.01691	-1.7718	1.049
2165	1595	0.02569	-1.5903	1.040

Run No. (10)

1/t = 0.2421 sec

(Methane) (uncorrected)	(Me_3SiH)	$k(sec^{-1})$	log k	$1/T \times 10^3 (^oK)$
916	1656	0.02479	-1.6057	1.033
1184	1577	0.03365	-1.4731	1.028
1396	1503	0.04162	-1.3807	1.020
1699	1405	0.05419	-1.2661	1.015

Full Kinetic Results

Hydrogen

Values of E ($kcal.mole^{-1}$)	Values of Log A	Run No.
80.0	16.0	1
80.2	15.8	2
80.0	16.1	3
80.3	16.2	4
80.2	15.6	5
80.1	16.1	6
80.4	15.8	7
80.5	16.3	8
80.3	15.8	9
80.7	16.1	10
81.1	16.1	11

Run No. (1)

$1/t = 0.2976$

(H_2) (uncorrected)	(Me_3SiH)	$k(sec^{-1})$	log k	$1/T \times 10^3 (^oK)$
771	765	0.0222	-1.6536	1.013
898	724	0.02731	-1.5636	1.006
1024	655	0.03443	-1.4634	1.000
1132	569	0.04381	-1.3584	0.9945

Run No. (2)

$1/t = 0.2976$

622	1289	0.01135	-1.945	1.014
753	1205	0.01471	-1.8324	1.007
835	1086	0.01809	-1.7426	1.002
896	1006	0.02090	-1.6799	0.9982

Run No. (3)

$1/t = 0.2976$

917	1341	0.03893	-1.4098	1.001
1105	1272	0.04946	-1.3058	0.9936
1282	1149	0.06348	-1.1974	0.9883
1428	984	0.0824	-1.0841	0.9828

Run No. (4)

1/t = 0.2976

(H_2) (uncorrected)	(Me_3SiH)	k(sec^{-1})	log k	1/T x 10^3(^oK)
875	1241	0.04011	-1.3968	1.003
1032	1163	0.05051	-1.2946	0.9964
1181	1055	0.06370	-1.1959	0.9918
1334	976	0.07776	-1.1093	0.9856

Run No. (5)

1/t = .0.2976

789	1757	0.01028	-1.9881	1.004
899	1477	0.01393	-1.8560	0.9964
1041	1325	0.01798	-1.7451	0.9892
1194	1123	0.02433	-1.6139	0.9819
1304	958	0.03115	-1.5065	0.9768
1350	851	0.03630	-1.4401	0.9722

Run No. (6)

1/t = 0.2891

838	1472	0.03241	-1.4894	1.004
995	1403	0.04037	-1.3939	0.9973
1196	1308	0.05201	-1.2839	0.9901
1370	1182	0.06593	-1.1809	0.9846
1573	1014	0.08941	-1.0486	0.9777
1740	916	0.1081	-0.9962	0.9740

Run No. (7)

1/t = 0.2421

1200	1300	0.01084	-1.9649	1.012
1394	1185	0.01381	-1.8598	1.004
1586	1060	0.0	-1.785	1.001

Run No. (8)

1/t = 0.2976

(H_2) (uncorrected)	(Me_3SiH)	k(sec^{-1})	log k	1/T x 10^3(^oK)
806	1628	0.02757	-1.5596	1.013
969	1579	0.03419	-1.4661	1.006
1137	1450	0.04368	-1.3597	1.001
1337	1312	0.05676	-1.2459	0.9927
1451	1191	0.06787	0.9892	
1617	1072	0.08401	-1.0756	0.9856
1750	932	0.1046	-0.9805	0.9795
1875	835	0.1251	-0.9028	0.9731

Run No. (9)

1/t = 0.2421

997	1453	0.008052	-2.0941	1.021
1193	1359	0.01031	-1.9868	1.015
1355	1245	0.01278	-1.8934	1.001
1605	1097	0.01717	-1.7653	1.001

Run No.(10)

1/t = 0.2891

703	1596	0.02506	-1.6011	1.002
863	1509	0.03256	-1.4873	0.9964
1058	1413	0.04259	-1.3707	0.9901
1214	1292	0.05347	-1.2719	0.9846
1366	1177	0.06604	-1.1802	0.9786
1524	1078	0.08042	-1.0946	0.9768
1678	990	0.09643	-1.0158	0.9731

Run No. (11)

1/t = 0.2976

685	1200	0.01344	-1.8716	1.014
769	1139	0.01589	-1.7988	1.010
847	1053	0.01892	-1.7230	1.006
917	937	0.02298	-1.6387	1.000

DISCUSSION

The aims of the discussion are twofold: to show the validity of the results, how they resolve some of the present confusion in the literature[2,3,4,5] and provide some basic information necessary for further investigations; and to explain what the results indicate about the nature of bonding to silicon.

Bond Dissociation Energy

For the process given by,

$$R_1R_2 + e \longrightarrow R_1^+ + \dot{R}_2 + 2e$$

$$A.P.(R_1^+) = D(R_1 - R_2) + I.P.(\dot{R}_1)$$

The measurement of $A.P.(R_1^+)$ can be used to calculate a value of bond dissociation energy in three ways:

1. by direct measurement of $I.P.(\dot{R}_1)$
2. by estimating or eliminating $I.P.(\dot{R}_1)$
3. by measuring $D(R_1 - R_2)$ by some means, combining it with $A.P.(R_1^+)$ to calculate $I.P.(\dot{R}_1)$ and then using this to find $D(R_1 - X)$ for a series of R_1X.

The $I.P.(Me_3Si)$ has not been determined directly and so the indirect methods 2. and 3. have been used in various forms to obtain $D(Me_3Si - X)$, with a consequent confusion in the reported values[2,3,4,5].

The bond dissociation energy values are discussed below, but first the validity of the A.P. measurements is established.

Appearance potentials were measured by an automatic method which used high sensitivity to concentrate on the threshold region

of the ionisation efficiency curves. The results are shown in table 4, together with those of other workers.

The values of the A.P. are lower than previously reported values, which, since A.P. measurements are likely to contain a certain amount of excess energy, makes the lower values more acceptable. All the measurements were carried out in accordance with Stevenson's rule[21] (see introduction), so that any excess energy is only likely to be excitational i.e. vibrational, rotational and electronic. Later in the discussion it will be shown that there is excellent agreement between the values of $D(Me_3Si - X)$ determined from the A.P.s and $D(Me_3Si - X)$ determined directly by a kinetic method, thus if any excitational energy is present it must be negligible.

It is interesting to note that the more recent the publication, the lower the values of A.P. reported, reflecting the trend (which the present work supports) of improvements in technique.

There is good agreement for A.P. (Me_3Si^+) from Me_6Si_2, Me_3SiH, and Me_4Si with the results of Haszeldine and co-workers[4]. They used the conventional method of Lossing[39] to interpret their results, so this is good supporting evidence for the method used in this work.

The appearance potentials of Me_2SiH^+ and Me_3Si^+, from Me_5Si_2H, may be used as a check on the consistency of the results by comparing them with the equivalent appearance potentials from Me_3SiH:

$$A.P.(Me_2SiH^+)_{Me_3SiH} - A.P.(Me_3Si^+)_{Me_3SiH} = 0.8 \text{ ev}$$

Compound	Ion	Standard	Appearance Potentials (ev) This Work	Ref.2	Ref.3	Ref.4
Me_6Si_2	Me_3Si^+	$i\text{-}C_5H_{12}^+$ *	10.0 ±0.1	10.69 ±0.04		10.0 ±0.1
Me_5Si_2H	Me_3Si^+	$i\text{-}C_5H_{12}^+$	9.9 ±0.1			
	Me_2SiH^+	$i\text{-}C_5H_{12}^+$	10.7 ±0.1			
Me_4Si	Me_4Si^+	$i\text{-}C_6H_{12}^+$	9.9 ±0.1	9.9 ±0.3		
	Me_3Si^+	$i\text{-}C_5H_{12}^+$	10.4 ±0.1	10.63 ±0.13	11.3 ±0.15	10.5 ±0.1
Me_3SiH	Me_3SiH^+	$i\text{-}C_5H_{12}^+$	9.6 (10.2)		9.8 ±0.3	
	Me_2SiH^+	$i\text{-}C_5H_{12}^+$	10.6 ±0.1	10.78 ±0.07	10.9 ±0.2	10.7 ±0.1
	Me_3Si^+	$C_2H_5Cl^+$	11.2 ±0.1	11.7 ±0.06	11.9 ±0.3	

* $n\text{-}C_3H_7Cl^+$ was also used with the same result

Table 4: Appearance Potential Measurements

Compound $Me_3Si - X$	$D(Me_3Si - X)$ kcal.mole^{-1} This Work	Ref.4	Ref.2	Ref.58	Ref.67
X = $SiMe_3$	67 ± 2 *	49 ± 6	86 ± 10		
$SiMe_2H$	65 ± 2				
Me	76 ± 2			78	
H	81 ± 2				81 ± 5

* kinetic value of Davidson and Stephenson[6]

Table 4.1: Bond Dissociation energies

which is exactly equal to:

$$A.P.(Me_2SiH^+)_{Me_3SiH^+} - A.P.(Me_3Si^+)_{Me_5Si_2H} = 0.8 \text{ ev.}$$

Having established the values of the A.P. measurements, the bond dissociation energies calculated from them are considered, together with the values determined by a kinetic method.

The results, together with those of other workers are shown in table 4.1. The values for $D(Me_3SiX)$ from the present work were calculated using the value of 67 ± 2 kcal.mole^{-1} for $D(Me_3Si - SiMe_3)$ in method 3 (above); reference (4) also used this method with their value of 49 ± 6 kcal.mole^{-1} for $D(Me_3Si - SiMe_3)$, and reference (2) used method 2 with an estimated value for $\Delta H_f^o(Me_6Si_2)_g$ of -126 ± 10 kcal.mole^{-1}.

The high value for $D(Me_3Si - SiMe_3)$[2] of 86 kcal.mole^{-1} (table 4.1) is due to the use of the value of $A.P.(Me_3Si^+)_{Me_6Si_2} = 10.69$ ev, which is 0.69 ev too high, (cf. result of this work and that of Haszeldine[4] et al. = 10.0 ev). Using the value of 10.0 ev, and $A.P.(Me_3Si^+)_{Me_4Si} = 10.4$ ev (lower than Hess's[2] value by 0.2 ev), together with the appropriate heats of formation, $D(Me_3Si - SiMe_3)$ may be recalculated:

$$Me_3Si - SiMe_3 \longrightarrow 2Me_3Si.$$

$$D(Me_3Si - SiMe_3) = \Delta H_1 = 2\Delta H_f^o(Me_3Si.)_g - \Delta H_f^o(Me_6Si_2)_g$$

(1) .... $Me_3SiSiMe_3 + e = Me_3Si^+ + Me_3Si. + 2e$, A.P.(1) = 10.0 ev

(2) .... $Me_4Si + e = Me_3Si^+ + Me. + 2e$, A.P.(2) = 10.4 ev

(2) - (1)

$$Me_3Si. + Me_4Si = Me. + Me_6Si_2 \quad , \quad \Delta H_2 = 0.4 \text{ ev} = 9.2 \text{ kcal.mole}^{-1}$$

and $$\Delta H_2 = \Delta H_f^o(Me_6Si_2) + \Delta H_f^o(Me.) - \Delta H_f^o(Me_4Si) - \Delta H_f^o(Me_3Si.)$$

i.e. $$9.2 = -126 + 33 + 69 - \Delta H_f^o(Me_3Si.)_g$$

$$\underline{\Delta H_f^o(Me_3Si.)_g = -33.2 \text{ kcal.mole}^{-1}}$$

Then $$D(Me_3Si - SiMe_3) = 2(-33.2) - (-126)$$

$$= \underline{60 \pm 10 \text{ kcal.mole}^{-1}}$$

Thus the redetermined value agrees well with the kinetic value of 67 kcal.mole^{-1} used in this work.

In comparing the value of 49 $\pm$ 6 kcal.mole^{-1} determined by Haszeldine et al[4], using the toluene carrier technique, with the value of 67 kcal.mole^{-1} determined by Davidson and Stephenson[6] using a conventional static system, it is necessary to see which value reflects most accurately the process initiated by the unimolecular dissociation of the (Si - Si) bond:

$$Me_3Si - SiMe_3 = 2Me_3Si. \quad , \quad Ea = D(Me_3Si - SiMe_3)$$

i.e. where processes which will lower the overall activation energy, Ea, e.g. chain reactions, heterogeneous behaviour, bimolecular reactions or reactions with gas-phase or adsorbed impurities, are absent.

Stephenson's report[6] shows that great care was taken over the experimental conditions; the stoichiometry was fully investigated

and, significantly, the temperature was kept below 555°C for 'at temperatures greater than this kinetic analysis could not be carried out because of the rapidity of the decomposition'. In comparison, the experiments of Haszeldine et al[4] were carried out over the temperature range 660 - 770°C, no detailed product analysis was given and no attempt was made at evaluating the stoichiometry. The experiments were carried out with at least 55% decomposition, at high temperatures, where they were no doubt complicated by the formation of (and abstraction by) methyl radicals, and the rapid decomposition of the various silyl radicals — as was indicated by the reported presence of methane, hydrogen and various alkylsilanes.

Therefore it seems reasonable to conclude that the value of 67 kcal.mole^{-1}, determined under more precise conditions, at lower temperatures and less than 5% decomposition, is more likely to relate to the unimolecular dissociation and D(Me_3Si - $SiMe_3$). Having established the values of A.P. and D(Me_3Si - $SiMe_3$), the values of D(Me_3Si - X) automatically follow. Further support to the values is given by:

1. Kerr et al[67], from studies of the reaction of methyl radicals with alkysilanes, have predicted a value for D(Me_3Si - H) as 81 ± 5 kcal.mole^{-1}.

2. The values for D(Me_3Si - X) determined by the indirect method using electron impact data are likely to be the upper limits of the true values, which should be reflected by direct kinetic determinations.

The work on the pyrolysis of trimethylsilane, as will be shown, has now confirmed this, the values:

$$D(Me_3Si - H) = 80.3 \pm 0.5 \text{ kcal.mole}^{-1}$$

$$D(Me - SiMe_2H) = 76.5 \pm 0.5 \text{ kcal.mole}^{-1}$$

giving excellent support to the conclusions reached from the electron impact work. The kinetic results are discussed more fully below, but first the electron impact results are completed with a discussion of the heats of formation.

Heats of formation

The values for the heats of formation of Me_3SiX are shown in table 4.2.

	$\Delta H_f^o(Me_3SiX)_g$ kcal.mole^{-1}		
Compound	This Work	Ref.2	Ref.60
Me_6Si_2	-118 ± 2	-126 ± 10	
Me_5Si_2H	-103 ± 2		
Me_4Si	- 68 ± 2		-69
Me_3SiH	- 55 ± 2		-60

Table 4.2: Heats of Formation

There is good agreement between the value for hexamethyldisilane, determined here, and the value of -126 kcal.mole^{-1}, calculated by Hess et al[2] using the group parameter method[61].

The values measured by Tannenbaum[60] show a lack of internal consistency which may be shown to lie in his value for $\Delta H_f^o(Me_3SiH)_g$:

considering the hypothetical reactions,

$$Me_2SiH_2 + Me_4Si = 2Me_3SiH \quad \ldots\ldots\ldots \Delta H_1$$

$$Me_2SiH_2 + Me. = Me_3SiH + H. \quad \ldots\ldots\ldots \Delta H_2$$

$$Me_3SiH + Me. = Me_4Si + H. \quad \ldots\ldots\ldots \Delta H_3$$

$$Me_2SiH_2 + 2Me. = Me_4Si + 2H. \quad \ldots\ldots\ldots \Delta H_4$$

Since the bonds broken and formed are very similar, ΔH_1 should be close to zero; in the analogous hydrocarbon reaction, where the bonds are more sensitive to environment, $\Delta H = 0.2$ kcal.mole^{-1}.

ΔH_2 and ΔH_3 can be evaluated from appearance potentials:

$$Me_2SiH_2 + e = Me_2SiH^+ + H. + 2e \qquad \text{A.P.(1)}$$

$$Me_3SiH + e = Me_2SiH^+ + Me. + 2e \qquad \text{A.P.(2)}$$

$$\Delta H_2 = \text{A.P.(1)} - \text{A.P.(2)} = \underline{0.24 \text{ ev}}^2 = \underline{5.5 \pm 2.0} \text{ kcal.mole}^{-1}$$

(Although the absolute values of A.P.(1) and A.P.(2) are doubtful, the difference between them is likely to be more reliable)

$$Me_3SiH + e = Me_3Si^+ + H. + 2e \qquad \text{A.P.(3)}$$

$$Me_4Si + e = Me_3Si^+ + Me. + 2e \qquad \text{A.P.(4)}$$

$$\Delta H_3 = \text{A.P.(3)} - \text{A.P.(4)} = \underline{0.2 \text{ ev}}^{10,4} = \underline{5.5 \pm 2.0} \text{ kcal.mole}^{-1}$$

Then $\Delta H_4 = 2\Delta H_2 - \Delta H_1 = \underline{11 \pm 2 \text{ kcal.mole}^{-1}}$

If these heats of reaction are recalculated directly from Tannenbaum's data, using the standard values for H. and Me., the results show that there is only agreement for ΔH_4:

$$\Delta H_1 = 2\Delta H_f^o(Me_3SiH)_g - \Delta H_f^o(Me_4Si)_g - \Delta H_f^o(Me_2SiH_2)_g$$
$$= -120 \qquad + 42 \qquad + 69 \quad \text{kcal.mole}^{-1}$$
$$= \underline{-9 \text{ kcal.mole}^{-1}}$$

By similar calculations $\Delta H_2 = 0$, $\Delta H_3 = +9$ and $\Delta H_4 = +9.2$ kcal.mole^{-1} respectively. If the value for $\Delta H_f^o(Me_3SiH)_g$ is modified by 4.5 kcal.mole^{-1} to 55.5 kcal.mole^{-1}, the discrepancies in ΔH_1, ΔH_2, and ΔH_3 disappear. With this modification Tannenbaum's data agrees extremely well with those found in this work.

Kinetic values of bond dissociation energy

Evaluation of the flow system

The work on di-t-butyl peroxide (DTBP) was carried out in order to establish the experimental technique: the stirred-flow reactor was operated at a series of pressures and flow rates, and a method was developed which allowed all the necessary data for an Arrhenius plot to be collected in one experiment:

The parameters found for the pyrolysis of DTBP:

$$[(Me_3CO)]_2 \xrightarrow{k} (Me)_2CO + C_2H_6$$

are shown in table 4.3, together with the results of other workers. The result gave very good agreement with the literature and so established the necessary confidence in the method.

Method	Temp.Range °K	Gas Present	A x 10^{16} (sec^{-1})	E(kcal.$mole^{-1}$)	ref.
Flow	500 - 520	N_2	0.11	36.1	This work
Flow	450 - 545	Toluene	0.07	36.0	62
Flow	555 - 625	Helium	0.5	37.4	63
Flow	433 - 551	CO_2	1.2	38.3	50
Static	400 - 450	Nil	0.13	37.0	64

Table 4.3: Arrhenius Parameters for Di-t-butyl Peroxide

Pyrolysis of Trimethylsilane, Me_3SiH

Trimethylsilane was pyrolysed using the method as tested on DTBP, with modifications which enabled a more accurate measurement of the concentrations to be made (each peak height was recorded nine times and the average taken).

The results gave:

$$k_1(sec^{-1}) = 10^{15.84 \pm 0.5} \exp^{-76,500 \pm 500/RT}$$

(methane formation)

$$k_{1'}(sec^{-1}) = 10^{15.99 \pm 0.5} \exp^{-80,300 \pm 500/RT}$$

(hydrogen formation)

The following reaction scheme, consistent with the kinetic parameters and products, is proposed[65]:

$$Me_3SiH \longrightarrow Me. + Me_2\dot{S}iH \quad \ldots\ldots\ldots\ldots \quad (1)$$

$$Me. + Me_3SiH \longrightarrow CH_4 + Me_3Si. \quad \ldots\ldots\ldots\ldots \quad (2)$$

$$Me_3SiH \longrightarrow H. + Me_3Si. \quad \ldots\ldots\ldots\ldots \quad (1')$$

$$H. + Me_3SiH \longrightarrow H_2 + Me_3Si. \quad \ldots\ldots\ldots\ldots \quad (2')$$

$$Me_3Si. + Me_3SiH \longrightarrow Me_3SiH + .CH_2SiMe_2H \quad \ldots\ldots\ldots\ldots \quad (3)$$

$$.CH_2SiMe_2H \longrightarrow (CH_2SiMeH) + Me. \quad \ldots\ldots\ldots\ldots \quad (4)$$

$$\longrightarrow (CH_2SiMe_2) + H. \quad \ldots\ldots\ldots\ldots \quad (4')$$

The species in (4), (4') could either be a biradical or a short-lived molecule $CH_2 = SiMeH$ (or $CH_2 = SiMe_2$). The various products are then formed by radical combinations or insertions[67,68,69], as is shown below.

The reaction scheme is therefore formally a chain mechanism and so it would appear doubtful to identify the activation energies with $D(Me_3Si - H)$ and $D(Me_2HSi - Me)$. This would be true if there was a significant contribution to the formation of hydrogen and methane from the chain sequence, however this is not so, since the steady state treatment shows that the dominant term in the complex rate equation is $k_1'(Me_3SiH)$, or $k_1(Me_3SiH)$, for hydrogen and methane formation respectively (compare the example given in the introduction). Consider a simple scheme for hydrogen formation (a similar scheme can be derived for methane, with the same result):

$$Me_3SiH \xrightarrow{k_{1'}} Me_3Si. + H. \quad \ldots\ldots\ldots\ldots \quad (1')$$

$$H. + Me_3SiH \xrightarrow{k_2} H_2 + Me_3Si. \quad \ldots\ldots\ldots\ldots \quad (2')$$

$$Me_3Si. + Me_3SiH \xrightarrow{k_3} Me_3SiH + .CH_2SiHMe \quad \ldots\ldots\ldots \quad (3)$$

$$.CH_2SiHMe_2 \xrightarrow{k_{4'}} CH_2SiMe_2 + H. \quad \ldots\ldots\ldots\ldots \quad (4')$$

$$Me_3Si. + .CH_2SiHMe_2 \xrightarrow{k_5} Me_3SiCH_2SiHMe_2 \quad \ldots\ldots\ldots\ldots \quad (5)$$

A. $$\frac{d(Me_3Si.)}{dt} = k_{1'}(Me_3SiH) + k_2(H.)(Me_3SiH) - k_3(Me_3Si.)(Me_3SiH) - k_5(Me_3Si.)(.CH_2SiHMe_2) = 0 \text{ (steady state)}$$

B. $$\frac{d(H.)}{dt} = k_{1'}(Me_3SiH) - k_2(H.)(Me_3SiH) + k_{4'}(.CH_2SiHMe_2) = 0 \text{ s.s.}$$

C. $$\frac{d(.CH_2SiHMe_2)}{dt} = k_3(Me_3Si.)(Me_3SiH) - k_{4'}(.CH_2SiHMe_2) - k_5(Me_3Si.)(.CH_2SiHMe_2) = 0 \text{ s.s.}$$

A. + B. + C. $$2k_{1'}(Me_3SiH) = 2k_5(Me_3Si.)(.CH_2SiHMe_2)$$

$$(Me_3Si.) = \frac{k_{1'}(Me_3SiH)}{k_5(.CH_2SiHMe_2)}$$

Substitute in C

$$\frac{k_{1'}k_3(Me_3SiH)^2}{k_5(.CH_2SiHMe_2)} - k_{4'}(.CH_2SiHMe_2) - k_{1'}(Me_3SiH) = 0$$

$$k_{4'}k_5(.CH_2SiHMe_2)^2 + k_{1'}k_5(Me_3SiH)(.CH_2SiMe_2H) - k_1k_3(Me_3SiH)^2 = 0$$

Soln. of the simultaneous equation gives:

$$(.CH_2SiHMe_2) = \frac{-k_1,k_5(Me_3SiH)+\left\{\left[k_1,k_5(Me_3SiH)\right]^2+4k_1'k_3k_4,k_5(Me_3SiH)^2\right\}^{\frac{1}{2}}}{2k_4,k_5}$$

Substitute in B

$$k_1,(Me_3SiH) - k_2(H.)(Me_3SiH) + k_4,(.CH_2SiHMe_2) = 0$$

$$(H.) = \frac{k_1,(Me_3SiH) + k_4(.CH_2SiHMe_2)}{k_2(Me_3SiH)}$$

$$\frac{d(H_2)}{dt} = k_2(H.)(Me_3SiH) = k_1,(Me_3SiH) + k_4,(.CH_2SiMe_2)$$

where $k_4,(.CH_2SiMe_2H)$ is the contribution from the chain reaction.

$$\text{Thus } \frac{d(H_2)}{dt} = k_1,(Me_3SiH) + \left[\frac{-k_1'}{2} + \left(\frac{k_1'^2}{4} + \frac{k_1,k_4,k_3}{k_5}\right)^{\frac{1}{2}}\right](Me_3SiH)$$

Substituting the estimated values of the rate constants, from table 4.4:

$$\frac{d(H_2)}{dt} = k_1,(Me_3SiH) + (-7.95 \times 10^{-3} + 7.95 \times 10^{-3})(Me_3SiH)$$

$$= \underline{k_1,(Me_3SiH.)}$$

The result of the steady state treatment means that the activation energies of the chain steps 4 and 4' are sufficiently high to be energetically unfavourable compared to the initial steps, so that they do not contribute significantly to the formation of hydrogen. The contribution to the hydrogen formation by steps 3 and 4' was in fact zero in the simple chain scheme shown above, since the stoichiometry

was assumed as 2 moles $Me_3SiH \longrightarrow$ 1 mole H_2, and thus $\frac{d(H_2)}{dt} = k_1'(Me_3SiH)$; however, if the exact stoichiometry was known, the rate of formation of hydrogen would be given by:

$\frac{d(H_2)}{dt} = ak_1'(Me_3SiH)$, where $1 < a < 2$, and there would then be a small, but still insignificant, contribution from the chain. (This point is discussed later.)

A similar scheme to the above for Me_3SiH is likely to apply to the pyrolysis of tetramethylsilane, by Helm and Mack[59]. They report Arrhenius parameters consistent with the fission of the silicon-methyl bond, for extensive decomposition of the compound.

The result is therefore in contrast to the similar pyrolysis of hydrocarbons, where steps such as 3 and 4' have lower activation energies, and occur very readily, contributing significantly to the product formation. An example is the pyrolysis of ethane which, in the temperature range 800 - 1000°K, gives principally ethylene and hydrogen. A simplified Rice-Herzfeld scheme is[66]:

$C_2H_6 \xrightarrow{1} 2\dot{C}H_3$	$k_1 = 10^{21} exp^{-88000/RT}$
$.CH_3 + C_2H_6 \xrightarrow{2} CH_4 + .C_2H_5$	$k_2 = 10^{11} exp^{-10400/RT}$
$.C_2H_5 \xrightarrow{3} C_2H_4 + H.$	$k_3 = 10^{16} exp^{-40600/RT}$
$H. + C_2H_6 \xrightarrow{4} C_2H_5 + H_2$	$k_4 = 10^{12} exp^{-6400/RT}$
$2C_2H_5 \xrightarrow{5} C_2H_4 + C_2H_6$	$k_5 = 10^{13} exp^{-900/RT}$
$\xrightarrow{5'} C_4H_{10}$	$k_5' = 10^{13} exp^{-0/RT}$

where $\frac{d(CH_4)}{dt} = 2k_1(C_2H_6)$ and corresponds to $\frac{d(H_2)}{dt} = k_1'(Me_3SiH)$;

steps 3 and 4 correspond to steps 4' and 3 (in pyrolysis of Me_3SiH), but have activation energies lower by 9.4 and 20.6 kcal.mole^{-1} respectively.

Steps 3 and 4 are now particularly favourable energetically and occur very readily such that ethylene and hydrogen are formed in greater quantities than methane (from a non-chain step). Thus the steady state treatment gives complex rate equations for the formation of ethylene and hydrogen, with the significant terms coming from the chain steps.

The activation energies of the processes leading to methane and hydrogen formation are therefore identified with the bond dissociation energies of the (Si - C) and (Si - H) bonds in trimethylsilane, thus:

$$D(Me_2HSi^{\bullet} - Me) = 76.5 \pm 0.5 \text{ kcal.mole}^{-1}$$

$$D(Me_3Si - H) = 80.3 \pm 0.5 \text{ kcal.mole}^{-1}$$

Rate constants used in the steady state treatment for hydrogen

The rate constants are shown in table 4.4.

Reaction	A factor (units as k)	Activation Energy (kcal.mole^{-1})	log k @ 1000°K^{-1} (1st order sec^{-1} 2nd order cc mole^{-1}sec^{-1})	ref.
(1')	16.0	80.3	-1.8	This work
(3)	11.0	27	+5.1	Estimated
(4')	14	50	+3.1	"
(5)	13.5	2	+13.1	"

Table 4.4: Values of parameters used in S.S. equation

(i) The rate constant for (3) was evaluated from considerations of the reaction:

$$Me_3Si. + Me_3SiH \underset{(-3)}{\overset{(3)}{\rightleftharpoons}} Me_3SiH + .CH_2SiHMe_2$$

The closest known analogy to (-3) is the attack of Me. on trimethylsilane: $Me. + Me_3SiH \xrightarrow{k} CH_4 + Me_3Si.$

for which Kerr[67] reports a value of $k = 10^{11}e^{-7000/RT}$. By considering $.CH_2SiHMe_2$ as a substituted methyl radical, and taking into account its greater bulk, $k_{(-3)}$ was estimated as, $k_{(-3)} = 10^{10}e^{-9000/RT}$. The change in entropy, ΔS, for $Me_3Si. \longrightarrow .CH_2SiHMe_2$ corresponds to $\frac{A_3}{A_{-3}} \simeq 10$, and the difference between the energy of the bonds broken and the bonds formed is: $D(RCH_2 - H) - D(Me_3Si - H) = 98 - 80 = 18$ kcal.mole^{-1}, thus $k_3 = 10^{11}e^{-27000/RT}$.

(ii) $.CH_2SiMe_2H \xrightarrow{k_{4'}} (CH_2SiMe_2) + H.$

The analogous reaction to 4' is the olefin elimination[11]:

$$CH_2 - CHMe_2 \longrightarrow CH_2 = CMe_2 + H.$$

Compared to the olefin, CH_2SiMe_2 will be very much less stable, either as a biradical, $\dot{C}H_2SiMe_2\dot{}$ or as the unstable, short-lived molecule $CH_2 = SiMe_2$. Thus $k_{4'}$ is estimated as, $k_{4'} = 10^{14}e^{-50000/RT}$.

(iii) By analogy with the many radical combinations reported in the literature, the rate constant of (5) was estimated as $k_5 = 10^{13.5}e^{-2000/RT}$, the small activation energy being included to take account of the size of the radicals.

Products

The products were identified by mass spectrometry (see results section) as disilanes, disilamethylenes and disilacyclobutanes, with very small amounts of dimethyl- and tetramethyl-silanes. No polymeric products were found.

Ratio of Products

The ratio of the rate constants, $\frac{k_{CH_4}}{k_{H_2}}$ was found to be approximately 5, (5.3 at the bottom of the temperature range to 5.0 at the top). This result, together with the assumption of a perfect silicon balance (total amount of silicon present is constant), which is reasonable in view of the simplicity of the products (above), and the approximate stoichiometry of 2 moles trimethylsilane $\longrightarrow$ 1 mole methane, and hydrogen respectively, allows the approximate ratio of the products to be deduced:

$$Me_3SiH \longrightarrow CH_4 + H_2$$

but methane and hydrogen are formed in the ratio 5 : 1, thus this becomes;

$$12\ Me_3SiH \longrightarrow 5CH_4 + H_2$$

which with the perfect silicon balance means that the products other than hydrogen and methane must contain 12 Si atoms, neglecting the very small amounts of dimethyl- and tetramethyl-silanes, the disilicon compounds therefore must form 6 moles and 50% of the product total.

Ratio of (CH_2SiMe_2) : (CH_2SiMeH)

Assuming that the mass spectrometer has equal sensitivities to each of the silacyclobutanes (this is reasonable in view of their close similarity), the molecular peak heights m/e 144, 130, and 116 respectively, will give an approximate measure of the amounts of CH_2SiMe_2 and CH_2SiMeH present. From the reaction scheme the concentrations are given by:

$$(CH_2SiMe_2) = 2(144) + \left(\frac{130}{2}\right)$$

$$(CH_2SiMeH) = 2(116) + \left(\frac{130}{2}\right)$$

The ratio, from a series of mass spectra, is shown in table 4.5.

m/e	Peak height	Peak height	Peak height	Peak height
144	3	2	4	4
130	25	12.5	44	37
116	36	24	49	40
(CH_2SiMe_2) : (CH_2SiMeH)	1 : 5	1 : 5	1 : 4	1 : 4

Table 4.5: Ratio CH_2SiMe_2 : CH_2SiMeH

The result (considering the uncertainties) gives reasonable agreement with the value predicted from the experimental ratio of rate constants, $\frac{k_1}{k_{1'}} \simeq 5$.

Formation of products

The formation of the products can be readily described in terms of simple radical reactions e.g. dimerisation of $Me_2\dot{S}iH$, and $Me_3Si.$ respectively, to form the disilanes, $HMe_2SiSiMe_2H$ and $Me_3SiSiMe_3$. The full set of radical reactions are shown in table 4.6.

Radical Reaction	Product	Type
Combination		
$Me_2\dot{S}iH + Me_3Si.$	$HMe_2SiSiMe_3$	disilane
$Me_2\dot{S}iH + .CH_2SiHMe_2$	$HMe_2SiCH_2SiHMe_2$	disilamethylene
$Me_3Si. + .CH_2SiHMe_2$	$Me_3SiCH_2SiHMe_2$	disilamethylene
$(CH_2SiMeH)+(CH_2SiMe_2)$	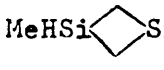	disilacyclobutane
Dimerisation		
$2Me_2\dot{S}iH$	$HMe_2SiSiMe_2H$	disilane
$2Me_3Si.$	$Me_3SiSiMe_3$	disilane
$2CH_2SiHMe_2$	$HMe_2SiCH_2CH_2SiHMe_2$	disilaethylene
$2(CH_2SiMe_2)$	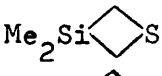	disilacyclobutane
$2(CH_2SiHMe)$	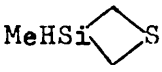	disilacyclobutane
Insertion		
$Me_3SiH + (CH_2SiMe_2)$	$Me_3SiCH_2SiMe_2H$	disilamethylene
$Me_3SiH + (CH_2SiMeH)$	$Me_3SiCH_2SiMeH_2$	disilamethylene

Table 4.6: Radical reactions for product formation

There is increasing evidence in the literature for radical insertion reactions of the type shown in table 4.6, for the formation of the disilamethylenes $Me_3SiCH_2SiMe_2H$ and $Me_3SiCH_2SiMeH_2$ (isomeric with $Me_2HSiCH_2SiMe_2H$). Skell and Goldstein[68] studied the reaction of dimethylsilene with trimethylsilane and found insertion:

$$Me_2\ddot{S}i + Me_3Si\text{-}H \longrightarrow Me_3SiSiMe_2H$$

Strauz[69] et al proposed a similar scheme for the reaction of methylsilene with methylsilane:

$$MeH\ddot{S}i + MeSiH_3 \longrightarrow MeH_2SiSiMeH_2$$

<u>Ch_2SiMe_2 and CH_2SiMeH</u>

It is not possible to say categorically whether the species are unstable, short-lived molecules containing a (Si = C), $P_\pi - P_\pi$ bond or whether they are biradicals. The literature contains qualitative evidence for both possibilities: Nametkin et al[70], from studies on the pyrolysis of a number of 1,1-disubstituted-1-silacyclobutanes, proposed the formation of $CH_2 = SiR_2$ as an unstable intermediate; and similar work by Flowers and Gusel'nikov[71] gave $CH_2 = SiMe_2$ as an intermediate in the formation of 1,1,3,3,-dimethyldisilacyclobutane (II):

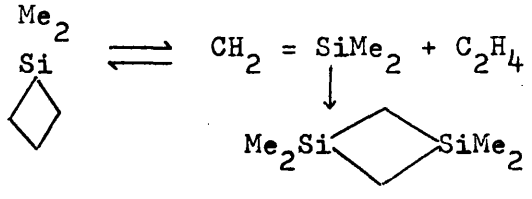

(II)

Frtiz[57] found (II) in the pyrolysis products of Me_4Si and suggested

that it was formed by the dimerisation of the biradicals:

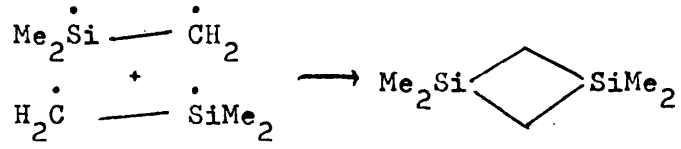

Frequency factors (A factors)

The values of the frequency factors fit into the category which are called 'abnormally high', a rather erroneous title since many such A factors have been reported for unimolecular dissociations. The values have been called 'abnormal' since they cannot be explained by the classical theories (Kassel[72], Rice and Ramsperger[73], and Slater[74]) which all derived an expression $k_\infty = A_\infty e^{-e_o/RT}$ where A was closely related to the vibrational frequencies of the molecule and usually had a value of about $10^{13} sec^{-1}$.

More recently Steele and Laidler[75] have considered the problem by relating the frequency factor to the positive entropies of the dissociation reaction. They concluded that dissociations with high frequency factors involved large increases in entropy due to a softening of certain vibrations in the activated complex, the loose vibrations ultimately becoming translational and rotational motions. By the same token a 'normal' A factor would be associated with dissociation involving a tightly-bound activated complex. The theory gives a good qualitative explanation and can be applied to dissociations in which either one or two bonds are broken; examples of the latter have been reported by Benson and De More[76] e.g. the decompositions of azo compounds. The explanation of the 'abnormal'

A factors for dissociations in which two bonds are broken is more obvious, since the activated state will clearly be of higher entropy than the initial state.

The high values of the frequency factors found in this work are not consistent with molecular elimination:

$$Me_3SiH \longrightarrow CH_4 + Me_2\ddot{Si}$$

$$Me_3SiH \longrightarrow H_2 + \dot{C}H_2Me_2\dot{Si}$$

which would proceed via tightly-bound transition states with low A factors, (for a list of A factors for molecular eliminations see reference 77).

It seems reasonable to conclude that the high A factors are characteristic of the unimolecular dissociations:

$$Me_3SiH \longrightarrow H. + Me_3Si.$$

$$\longrightarrow Me. + Me_2\dot{S}iH$$

Although the rates of formation of methane and hydrogen are determined by k_1 and $k_{1'}$, the exact rate equations, as was mentioned earlier, should probably be in the form:

$$\frac{d(CH_4)}{dt} = ak_1(Me_3SiH) \quad ; \quad \frac{d(H_2)}{dt} = bk_{1'}(Me_3SiH)$$

where a and b are constants with values between 1 and 2, depending on the detailed mechanism. This feature can be allowed for by extending the limits of uncertainty in the frequency factors:

$$k_1(sec^{-1}) = 10^{15.8 \pm 0.8} \exp^{-76500 \pm 500/RT} \quad ;$$

$$k_{1'}(sec^{-1}) = 10^{16 \pm 0.8} \exp^{-80300 \pm 500/RT}$$

From the discussion on entropy (above), one would expect that reaction (1') would have a lower A factor than (1); this would be so if b $\geq$ a.

The (Si - H) and (Si - C) bonds

The pyrolysis of trimethylsilane has yielded two bond dissociation energies, D(Me - $SiMe_2H$) = 80.3 $\pm$ 0.5 and D(H - $SiMe_3$) = 76.5 $\pm$ 0.5 kcal.mole^{-1} respectively, determined in the same experiments under identical conditions; the results therefore provide very firm evidence as to the relative strengths of the (Si - C) and (Si - H) bonds in trimethylsilane, and show that the (Si - H) bond is stronger than was previously thought and is definitely stronger than the (Si - C) bond.

Mares and Chvalovsky[78,79] have studied the pyrolyses of some alkyl- and aryl-silanes and have suggested homogeneous radical chain mechanisms in which the principal initiation step is cleavage of the (Si - H) bond, in contrast with the results from the kinetic and electron impact work in this thesis.

Mares and Chvalovsky[78,79] concentrated on identifying the products of the pyrolyses rather than performing a formal kinetic study and the experiments were carried out to extensive decomposition (of products as well as reactant), with formation of large amounts of polymers. The activation energies were not quoted but can be calculated from the published data to give values as shown below:

Reaction pyrolysis of:	$E^{78,79}$ (kcal.mole^{-1})
methyldiethylsilane	41.5
triethylsilane	33.5
triisobutylsilane	29.3
triisopropylsilane	27.9
phenyldimethylsilane	28.0

The conclusions of Mares and Chvalovsky[78,79] differ from ours only in interpretation: theirs is a qualitative explanation i.e. (Si - H) is the most labile bond in the compounds, whilst our quantitative data would indicate that this is not so. The extensive decomposition and consequent complex formation of products in their work makes it practically impossible to give a meaningful mechanism: the product formation can just as well be explained by a radical chain mechanism in which there are two principal initiation steps, i.e. cleavage of (Si - alkyl), and (Si - H) bonds respectively. The silyl radical would then be formed not only by dissociation of (Si - H) bond but also by the hydrogen abstraction reaction:

$$R\cdot + R_3SiH \longrightarrow RH + R_3Si\cdot$$

which, as was shown earlier, occurs much faster than the analogous hydrocarbon reaction, and is a large source of the R_3Si radicals.

The activation energies, whilst possibly being consistent with complex homogeneous chain reactions, also fall in the range which has been found by workers in our laboratory for heterogeneous

reactions: our experience has shown that considerable care must be taken in order to prevent heterogeneous behaviour in the pyrolyses of organosilicon compounds. In the past the desired homogeneous conditions have been achieved by repeatedly exposing the reaction vessel to the reactant or some other reagent that will produce an inert carbon carbon coating on the surface. The work in this thesis, and the recent work of Stephenson[6], has shown that if oxygen can be entirely eliminated from the system then elaborate treatment of the vessel surface is not necessary, indicating that the heterogeneous reaction may be a chemisorption process at oxygen-active sites on the surface of the vessel.

The activation energies for the heterogeneous reactions of some organosilicon compounds are shown below, and it can be seen that the values are very similar to those found by Mares and Chvalovsky.

Reaction pyrolysis of:	E ($kcal.mole^{-1}$)	Reference
2-chloroethyltrimethylsilane	29.6	80
2-hydroxyethyltrimethylsilane	29.2	80
Trichlorosilane + chlorobenzene	26.5	81
Trimethylsilane	27.0	This work

It seems likely, therefore, that the reactions studied by them contained a substantial heterogeneous component, which, since the rates of the reactions were independent of the surface area, must have affected the initiation and termination steps equally; however, a

detailed kinetic study would be required to clarify their results quantitatively.

Summary

The values of activation energy determined in the kinetic study on Me_3SiH have been identified with D(Me - $SiMe_2H$) and D(H - $SiMe_3$), as 76.5 ± 0.5 and 80.3 ± 0.5 kcal.mole^{-1} respectively. The results therefore agree extremely well with those of the electron impact study: D(Me - $SiMe_3$) = 76 ± 2 kcal.mole^{-1}, D(H - $SiMe_3$) = 81 ± 2 kcal.mole^{-1}, and thus give very good evidence as to the reliability of the electron impact work. The agreement means that the A.P.s give the same results for $\Delta H_f^o(Me_3SiX)_g$ and D(Me_3Si - X) when used in conjunction with the results of two independent kinetic studies: this work and that of Davidson and Stephenson[6], for D(Me_3Si - $SiMe_3$). Thus the most reliable values of heats of formation and bond dissociation energies of the organosilanes, Me_3SiX, X = Me_3Si, Me_2SiH, Me, H, are:

Compound	$\Delta H_f^o(Me_3SiX)_g$ (kcal.mole^{-1})	D(Me_3Si - X)	Reference
$Me_3SiSiMe_3$	-118 ± 2	67.3 ± 2 *	This work[10,65]
$Me_3SiSiMe_2H$	-103 ± 2	65 ± 2	"
Me_4Si	- 68 ± 2	76 ± 2	"
Me_3SiH	- 55 ± 2	80.3 ± 0.5	"
Me - $SiMe_2H$		76.5 ± 0.5	"

* kinetic value of Davidson and Stephenson[6].

Comparisons with carbon

The ionisation potentials of the molecules Me_3SiH, Me_4Si and radicals $Me_3Si.$ and $Me_2\dot{S}iH$, together with their carbon analogues are shown in table 4.7.

	M = Si	M = C[48]
Me_3MMe	9.9	10.3
Me_3MH	(9.6)	10.6
$Me_3M.$	7.1	7.4
$Me_2\dot{M}H$	7.9	8.7

Table 4.7: Ionisation Potentials

The molecular ions are present in the mass spectra of these compounds in low abundance and so the results will not be so accurate as those for the other characteristic ions. The values for the silicon compounds exhibit a similar trend to the t-butyl analogues, being lower in value as would be expected from a comparison of the ionisation potentials of carbon and silicon.

The only equivocal result is I.P.(Me_3SiH^+), a value of 9.6 ev was obtained on some occasions and 10.2 ev on others. The reason for the discrepancy is probably because the low intensity of Me_3SiH^+ was sufficient to make the ion undetectable down to the true threshold, the ion, in effect, disappearing 'early'.

The bond dissociation energies of Me_3SiX and carbon analogues are shown in table 4.8 below.

X	$D(Me_3Si - X)$	$D(Me_3C - X)$[16]
Me_3Si	67	68
Me	76	81
H	80	91

values in kcal.mole^{-1}, rounded to nearest whole number.

Table 4.8: Bond Dissociation Energies

The silicon compounds again exhibit the expected trends with their carbon analogues. It can be seen from the table that the t-butyl group (Me_3C-) is progressively more strongly bonded to Me and H than is trimethylsilyl (Me_3Si-), although $D(Me_3Si - SiMe_3)$ and $D(Me_3C - CMe_3)$ are very similar. The large increase in D with decreasing size of the attached group: 23 kcal.mole^{-1} difference between $D(Me_3C - H)$ and $D(Me_3C - CMe_3)$, compared to only 13 kcal.mole^{-1} between $D(Me_3Si - H)$ and $D(Me_3Si - SiMe_3)$, reflects the difficulty which Me_3C- has in accommodating bulky groups. The reason Me_3Si- does not experience the effect must be due to the larger size of the silicon atom: covalent radius of silicon = 1.17 Å, C = 0.77 Å [82]. Thus, in this respect, Me_3Si- represent H_3C- more closely than Me_3C-, for with the former pair the attached groups are smaller than the central atom and will not cause steric hindrance.

Recently Gowenlock[83] has compared the difference $D(H_3C - X) - D(Me_3C - X)$ with $D(H_3Si - X) - D(Me_3Si - X)$ and has suggested that

there is a similar stabilisation of $Me_3Si.$ to that of $Me_3C.$ The latter is said to be stabilised by resonance energy as shown in (I) and so the equivalent for $Me_3Si.$ would involve a $P_\pi - P_\pi$ double bond (II):

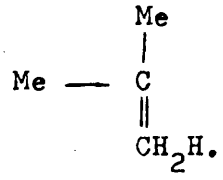

(I)

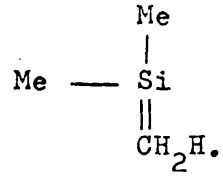

(II)

The type of structure as in (II) has already been mentioned in connection with the product formation (see kinetic sequence), but it would, as Gowenlock[83] points out, require a detailed E.S.R. study for clarification.

Electronegativity of silicon

Calculations have shown that Pauling's well known bond energy equation[84] has little basis on molecular orbital or valence bond grounds[85,88,89], and it has been criticized for the disagreements between its predictions and the experimental facts[90,91]. Its most important application has been to establish values of the average electronegativities of the elements, and we have used the equation in this respect to calculate the apparent electronegativity of silicon[10]. The values of $D(Me - SiMe_2H)$ and $D(H - SiMe_3)$ were used to compare the electronegativity differences, Δ, between silicon and carbon and silicon and hydrogen.

For Me_4Si,

$$\Delta = D(Me_3Si - Me) - \left[D(Me_3Si - SiMe_3) \times D(Me - Me) \right]^{\frac{1}{2}}$$

$$= 76 - (67 \times 88)^{\frac{1}{2}}$$

$$= \underline{0.8 \pm 2 \text{ kcal.mole}^{-1}}$$

Similarly, for Me_3SiH,

$$= D(Me_3Si - H) - \left[D(Me_3Si - SiMe_3) \times D(H - H) \right]^{\frac{1}{2}}$$

$$= 80 - (67 \times 104)^{\frac{1}{2}}$$

$$= \underline{-2.5 \pm 2 \text{ kcal.mole}^{-1}}$$

Thus Δ is approximately zero in each, which means that the electronegativity of silicon is approximately equal to that of hydrogen and carbon, i.e. it lies between 2.1 and 2.5 on the Pauling scale.

Pauling's method was originally derived for diatomic molecules in terms of their bond dissociation energies, and then extended to polyatomics by use of average bond energies, E. Because of the uncertainties involved in E values, the compounds were treated as quasi-diatomics: (Me_3Si) - (Me) and (Me_3Si) - (H), in the above calculations, and their D values used.

Thus if the prediction from the Pauling equation is correct, then (Si - C) and (Si - H), in Me_3SiX at least, are a lot less polar than was supposed.

Future work

At present the flow system is being used to study the pyrolysis of tetramethylsilane, which by analogy with trimethylsilane would be expected to proceed:

$$Me_4Si \xrightarrow{k} Me\cdot + Me_3Si\cdot$$

$$Me\cdot + Me_4Si \longrightarrow \cdot CH_2SiMe_3 + CH_4$$

The rate constant, k, can be obtained by measuring the rate of formation of methane, and this should lead to a precise value for $D(Me - SiMe_3)$.

The appearance potential technique has been continuously refined and improved, such that with the basic information that is now available from this work, bond dissociation energies for a wide range of compounds can be obtained.

REFERENCES

(1) T. L. Cottrell, 'The Strengths of Chemical Bonds', 2nd Edn., 1958, Butterworths, London.

(2) G. G. Hess, F. W. Lampe, and L. H. Sommer, J.Amer.Chem.Soc., 85, 23, (1965).

(3) B. G. Hobrock and R. W. Kiser, J.Phy.Chem., 66, 155, (1962).

(4)(a) J. A. Connor, G. Finney, G. J. Leigh, R. N. Haszeldine, P. J. Robinson, R. D. Sedgwick, and R. F. Simmons, Chem.Comm., 178, (1966).

(b) J. A. Connor, R. N. Haszeldine, G. J. Leigh, and R. D. Sedgwick, J.Chem.Soc.(A), 768, (1967).

(5) M. F. Lappert, J. B. Pedley, and P. N. K. Riley, Chem.Soc. Autumn Meeting (1966).

(6) I. M. T. Davidson and I. L. Stephenson, J.Chem.Soc.(A), 282, (1968).

(7) I. L. Stephenson, Ph.D. thesis, University of Leicester,(1967)

(8) S. J. Band, I. M. T. Davidson, and C. A. Lambert, Chem. Comm., 723,(1967).

(9) S. J. Band, I. M. T. Davidson, and C. A. Lambert, J. Organometal.Chem., 12, 3, (1968).

(10) S. J. Band, I. M. J. Davidson, and C. A. Lambert, J.Chem.Soc.(A), 2068, (1968).

(11) J. A. Kerr and A. F. Trotman-Dickenson, Prog.Reac.Kinetics, 1, 113, (1961).

(12) E. L. Metcalfe, J.Chem.Soc., 3563, (1963).

(13) E. L. Metcalfe, and A. F. Trotman-Dickenson, J.Chem.Soc., 4620, (1962).

(14) M. Szwarc, Chem.Rev. 47, 75, (1950).

(15) M. Szwarc, Proc.Roy.Soc.(A), 207, 5, (1951).

(16) J. A. Kerr, Chem.Rev., 66, 465, (1966).

(17) S. W. Benson, J.Chem.Ed., 42, 502, (1965).

(18) F. H. Field and J. L. Franklin, 'Electron Impact Phenomena and the Properties of Gaseous Ions', Academic Press Inc., New York, (1957), P.86.

(19) H. D. Hagstrum, Rev.Mod.Phys., 23, 185, (1951).

(20) H. W. Washburn, and C. E. Berry, Phy.Rev., 70 559, (1946).

(21) D. P. Stevenson, Disc.Farad.Soc., 10, 35, (1951).

(22) J. Franck, Trans.Farad.Soc., 21, 536, (1926).

(23) E. U. Condon, Phys.Rev., 32, 858, (1928).

(24) H. D. Hagstrum, and J. T. Tate, Phys.Rev., 59, 343, (1941).

(25) H. M. Rosenstock, M. B. Wallenstein, A. L. Jahrhaftig, and H. Eyring, Proc.Natl.Acad.Sci.(U.S.), 38, 667, (1952).

(26) G. G. Hall, Proc.Roy.Soc.,(A) 205, 541, (1951).

(27) G. G. Hall, Trans.Farad.Soc. 49, 113, (1953).

(28) J. Lennard-Jones, and G. G. Hall, Proc.Roy.Soc.,(A) 213, 102, (1952).

(29) J. L. Franklin, J.Chem.Phys., 22, 1034, (1954).

(30) H. D. Smyth, Proc.Roy.Soc.(A) 102, 283, (1922).

(31) R. H. Vought, Phys.Rev., 71, 93, (1947).

(32) J. W. Warren, Nature, 165, 811, (1950).

(33) R. E. Honig, J.Chem.Phy., 16. 105, (1948).

(34) R. E. Fox, W. M. Hickman, D. J. Grove, and T. Kjeldaas, Rev.Sci.Instr., 26, 1101, (1955).

(35) J. D. Waldron, and K. Wood, 'Mass Spectrometry', Inst. of Petroleum, (1950), P.16.

(36) D. P. Stevenson, and J. A. Hipple, Phy.Rev., 62, 237, (1942).

(37) C. A. McDowell, 'Mass Spectrometry', McGraw-Hill Book Company, Inc., (1963), P.513.

(38) R. W. Kiser, 'Introduction to Mass Spectrometry and its Applications', Prentice-Hall, Inc., New York (1965) P.166.

(39) F. P. Lossing, A. W. Tickner, and W. A. Bryce, J.Chem.Phys., 19, 1254, (1951).

(40) J. D. Morrison, J.Chem.Phy., 21, 1767, (1953) and ibid., 22, 1219,(1954)

(41) R. W. Kiser, 'Introduction to Mass Spectrometry and its Applications', Prentice-Hall, Inc., New York, (1965) P.195.

(42) E. B. Jordan, and N. D. Coggeshall, J.App.Phys., 13, 539, (1942).

(43) A. Grummit, Proc. of Fifth MS9, Mass Spectrometry Users Conference, (1967), P.23.

(44) E. G. Johnson, and A. O. Nier, Phys.Rev., 91, 10, (1953).

(45) E. J. Gallegos and R. F. Klaver, J.Sci.Instr., 44, 427,(1967).

(46) F. H. Field, and J. L. Franklin, 'Electron Impact Phenomena, and the Properties of Gaseous Ions', Academic Press, Inc., New York, (1957), P.41.

(47) J. A. Beynon, 'Mass Spectrometry and its Application to Organic Chemistry', Elsevier, Amsterdam, (1960), P.463.

(48) V. I. Vedeneyer, L. V. Gurvich, V. N. Kondtat'yev, V. A. Medvedev, and Ye. L. Frankevich, 'Bond Energies, Ionisation Potentials and Electron Affinities', Arnold, London, (1966), P.151.

(49) R. W. Kiser, 'Introduction to Mass Spectrometry and its Applications', Prentice-Hall, Inc., New York, (1965),P.162.

(50) M. F. R. Mulcahy, and D. J. Williams, Austr.J.Chem., 14, 535, (1961)

(51) A.E.I. Technical Information Sheet A222, 'Sample Inlet Systems MS10'.

(52) G. R. Wilson, and A. G. Smith, J.Org.Chem., 26, 557, (1961).

(53) M. Kumada, M. Yamaguchi, Y. Yamamota, J. Nakajima, and K. Shiina, J.Org.Chem., 21, 1264, (1956).

(54) M. Kumada, M. Ishikawa, and S. Maeda, J.Organometal.Chem., 2(6), 478, 1964.

(55) A. E. Beezer, and C. T. Mortimer, J.Chem.Soc.,(A), 514, (1966).

(56) G. M. Harris, J.Phy.Chem., 51, 505, (1947).

(57) G. Fritz, D. Kummer, and G. Sonntag, Z.anorg.Chem., 342, 113, (1966),
and G. Fritz, H. Buhl, J. Grobe, W. Reeting, and F. Aulinger, Z.anorg.Chem., 312, 201, (1961).

(58) N. Ya. Chernyak, R. A. Khmel'nitskii, T. V. D'yakova, V. M. Vdovin and T. N. Arkhipova, J.Gen.Chem.U.S.S.R., 36(1), 99, (1966).

(59) D. F. Helm, and E. Mack Jr., J.Amer.Chem.Soc., 59, 60, (1936).

(60) S. Tannenbaum, J.Amer.Chem.Soc., 76, 1027, (1954).

(61) J. L. Franklin, Ind.Eng.Chem., 41, 1070, (1949).

(62) J. Muraski, J. S. Roberts, and M. Szwarc, J.Chem.Phy., 19, 698, (1951).

(63) F. P. Lossing, and A. W. Tickner, J.Chem.Phy., 20, 907,(1952).

(64) M. T. Jaquiss, J. S. Roberts, and M. Szwarc, J.Amer.Chem.Soc., 74, 6005, (1952).

(65) I. M. T. Davidson, and C. A. Lambert, Chem.Comm.

(66) S. H. Benson, 'The Foundations of Chemical Kinetics', McGraw-Hill Book Company, Inc., (1960), P.349

(67) J. A. Kerr, D. H. Slater, and J. C. Young, J.Chem.Soc.(A), 134, (1967).

(68) P. S. Skell, and E. J. Goldstein, J.Amer.Chem.Soc., 86, 1442, (1968).

(69) O. P. Strauz, K. Obi, and W. K. Duholte, J.Amer.Chem.Soc., 90, 5,. (1968).

(70) N. S. Nametkin, V. M. Vdovin, L. E. Gusel'nikov, and V. I. Zavyalov, Izvest.Akad.Nauk. S.S.S.R. Ser.Khim., 584, (1966).
and N. S. Nametkin, L. E. Gusel'nikov, V. M. Vdovin, P. L. Grinberg, V. I. Zavyalov, and V. D. Oppengeim, Docklady Akad.Nauk. S.S.S.R., 171, 630, (1966).

(71) L. E. Gusel'nikov, and M. C. Flowers, Chem.Comm., 864 (1967).

(72) L. S. Kessel, J.Phys.Chem., 32, 225, (1928).

(73) O. K. Rice, and H. C. Ramsperger, J.Amer.Chem.Soc., 49 1617, (1927), and ibid. 50, 617 (1928).

(74) N. B.Slater, Proc. Cambridge Phil.Soc., 35, 36, (1939).

(75) C. Steel, and K. J. Laidler, J.Chem.Phys., 34, 1827, (1961).

(76) S. W. Benson, and W. B. De More, Ann.Rev.Phys.Chem., 16, 397, (1965)

(77) S. H. Benson, 'Foundations of Chemical Kinetics', McGraw-Hill Book Company, Inc., (1960) P.258.

(78) F. Mares, and V. Chvalovsky, Coll.Czech.Chem.Comm., 32, 382, (1967)

(79) F. Mares and V. Chvalovsky, J.Organometal.Chem., 6,327,(1966).

(80) I. M. T.Davidson, M. R. Jones, and C. Pett, J.Chem.Soc.B, 937, (1967)

(81) I. M. T. Davidson, C. Eaborn, and C. J. Wood, J.Organometal Chem., 10, 401, (1967).

(82) F. A. Cotton, and G. Wilkinson, 'Advanced Inorganic Chemistry' Interscience, (1962), P.93.

(83) B. G. Gowenlock, and J. Stevenson, J.Organometal.Chem., 15, 503, (1968).

(84) L. Pauling, 'Nature of the Chemical Bond', Cornell University Press, Ithaca, New York, (1944), P.58.

(85) R. Ferreira, Adv.Chem.Phys., 13, 55, (1967).

(86) F. O. Rice, and K. F. Herzfeld, J.Amer.Chem.Soc., 56, 284, (1934).

(87) G. L. Esteban, J. A. Kerr, and A. F. Trotman-Dickenson, J.Chem.Soc., 3873, (1963) and ibid., 3879, (1963).

(88) R. S. Mulliken, J.Chem.Phys., 3, 573, (1935).

(89) R. G. Pearson, J.Chem.Phys., 17, 969, (1949).

(90) R. Ferreira, Nature, 219, 61, (1968).

(91) R. Pearson, Chem.Comm., 2, 65, (1968).